

## Subdominant CD8 T-Cell Epitopes Account for Protection against Cytomegalovirus Independent of Immunodomination<sup>∇†</sup>

Rafaela Holtappels,<sup>1\*</sup> Christian O. Simon,<sup>1</sup> Michael W. Munks,<sup>2‡</sup> Doris Thomas,<sup>1</sup> Petra Deegen,<sup>1</sup> Birgit Kühnapfel,<sup>1</sup> Torsten Däubner,<sup>1</sup> Simone F. Emde,<sup>1</sup> Jürgen Podlech,<sup>1</sup> Natascha K. A. Grzimek,<sup>1</sup> Silke A. Oehrlein-Karpi,<sup>1</sup> Ann B. Hill,<sup>2</sup> and Matthias J. Reddehase<sup>1</sup>

*Institute for Virology, Johannes Gutenberg University, 55131 Mainz, Germany,<sup>1</sup> and Department of Molecular Microbiology and Immunology, Oregon Health and Science University, Portland, Oregon 97239<sup>2</sup>*

Received 22 January 2008/Accepted 17 March 2008

**Cytomegalovirus (CMV) infection continues to be a complication in recipients of hematopoietic stem cell transplantation (HSCT). Preexisting donor immunity is recognized as a favorable prognostic factor for the reconstitution of protective antiviral immunity mediated primarily by CD8 T cells. Furthermore, adoptive transfer of CMV-specific memory CD8 T (CD8-T<sub>M</sub>) cells is a therapeutic option for preventing CMV disease in HSCT recipients. Given the different CMV infection histories of donor and recipient, a problem may arise from an antigenic mismatch between the CMV variant that has primed donor immunity and the CMV variant acquired by the recipient. Here, we have used the BALB/c mouse model of CMV infection in the immunocompromised host to evaluate the importance of donor-recipient CMV matching in immunodominant epitopes (IDEs). For this, we generated the murine CMV (mCMV) recombinant virus mCMV-ΔIDE, in which the two memory repertoire IDEs, the IE1-derived peptide 168-YPHFMPTNL-176 presented by the major histocompatibility complex class I (MHC-I) molecule L<sup>d</sup> and the m164-derived peptide 257-AGPPRYSRI-265 presented by the MHC-I molecule D<sup>d</sup>, are both functionally deleted. Upon adoptive transfer, polyclonal donor CD8-T<sub>M</sub> cells primed by mCMV-ΔIDE and the corresponding revertant virus mCMV-revΔIDE controlled infection of immunocompromised recipients with comparable efficacy and regardless of whether or not IDEs were presented in the recipients. Importantly, CD8-T<sub>M</sub> cells primed under conditions of immunodomination by IDEs protected recipients in which IDEs were absent. This shows that protection does not depend on compensatory expansion of non-IDE-specific CD8-T<sub>M</sub> cells liberated from immunodomination by the deletion of IDEs. We conclude that protection is, rather, based on the collective antiviral potential of non-IDEs independent of the presence or absence of IDE-mediated immunodomination.**

Allogeneic hematopoietic stem cell transplantation (HSCT) combined with donor lymphocyte infusion is a promising therapeutic option against hematologic malignancies (2, 29). Reactivated cytomegalovirus (CMV) infection resulting in CMV disease, in particular, interstitial pneumonia, is a frequent and severe complication (6, 18, 56). As shown by Emery (13) and reviewed recently by Wills et al. (65), the risk of HSCT-associated CMV disease is basically defined by the CMV status of transplantation donor (D) and recipient (R). The combination D<sup>-</sup>R<sup>-</sup> bears no intrinsic CMV risk, while the combinations D<sup>+</sup>R<sup>-</sup> and D<sup>-</sup>R<sup>+</sup> are at risk of reactivating latent CMV from the donor transplant and from recipient tissues, respectively. Although a combination D<sup>+</sup>R<sup>+</sup> is prone to an additive risk of reactivation, CMV disease nevertheless occurs less frequently in D<sup>+</sup>R<sup>+</sup> than in D<sup>-</sup>R<sup>+</sup>, indicating a protective effect of pre-existing donor immunity (13). That adoptive transfer of CMV-

specific CD8 memory T (CD8-T<sub>M</sub>) cells is a promising approach for preventing CMV reactivation and disease has been established in the murine CMV (mCMV) model (50, 53, 55, 60; reviewed in references 20 and 22) and was confirmed for human CMV (hCMV) in clinical trials (8, 10, 45, 57, 64).

A potential problem so far never investigated systematically is the impact of an antigenic mismatch between the donor-derived and the recipient-derived CMV variant in a D<sup>+</sup>R<sup>+</sup> combination. Obviously, antigenic mismatch is not an issue in a D<sup>+</sup>R<sup>-</sup> combination of HSCT, since here priming of the donor and infection of the recipient are by the same virus. In a D<sup>+</sup>R<sup>+</sup> combination, however, donor-CMV and recipient-CMV are likely to differ due to the individuality of the infection history. CMV is often acquired perinatally or in early childhood. So, donor and recipient have usually harbored their respective CMV variants for many years or even decades. They were most likely infected by different variants *ab initio*, and further divergence may have resulted from the accumulation of mutations during productive primary infection and during multiple intermittent recurrences later on. Thus, a D<sup>+</sup>R<sup>+</sup> combination may more precisely be written as D<sup>Var1</sup>R<sup>Var2</sup>. Although, of course, not all differences in the proteomes of CMV variants concern CD8 T-cell epitopes, antigenic mismatch is a realistic scenario as indicated by antigenic variance of hCMV clinical isolates (11, 32) as well as by CD8 T-cell epitope mutations detected in mCMV isolates from outbred mice (34). Clearly,

\* Corresponding author. Mailing address: Institute for Virology, Johannes Gutenberg University, Hochhaus am Augustusplatz, 55131 Mainz, Germany. Phone: 49 6131 39 34451. Fax: 49 6131 39 35604. E-mail: R.Holtappels-Geginat@uni-mainz.de.

‡ Present address: National Jewish Medical and Research Center, Howard Hughes Medical Institute, 1400 Jackson St., K512, Denver, CO 80206.

† Supplemental material for this article may be found at <http://jvi.asm.org/>.

<sup>∇</sup> Published ahead of print on 26 March 2008.

antigenic mismatch might weaken the protective effect of donor CD8-T<sub>M</sub> cells against the virus variant reactivated from the recipient.

This issue cannot be investigated in clinical trials. It is the strength of animal models to provide evidence-based predictions. The BALB/c mouse model of CD8 T-cell-based immunotherapy of CMV disease has already demonstrated its predictive value with regard to the fundamental principles involved (reviewed in references 20, 22, and 49). It is a convenient model as its CD8-T<sub>M</sub>-cell recognition repertoire is focused on two immunodominant epitopes (IDEs) derived from viral proteins immediate early 1 (IE1)-pp89/76 and m164-gp36.5 (27).

Here, we have modulated the “viral immunome” by functional inactivation of both IDEs through point mutations of the respective C-terminal major histocompatibility complex class I (MHC-I) anchor residues of the peptides in recombinant virus mCMV-ΔIDE. According to the concept of immunodomination (33), CD8 T cells specific for “weak” epitopes dominated by IDEs after infection with wild-type (WT) virus might get the chance to expand in absence of IDEs and account for protection. Although we could identify an epitope within open reading frame ORF *m145* that indeed profits from the deletion of IDEs, our data show that protection in a recipient infected with mCMV-ΔIDE is independent of whether donor CD8 T cells were educated in the absence or presence of IDEs. This indicated that protective activity is not significantly influenced by immunodomination but, rather, that redundancy of protective epitopes ensures protection also after deletion of IDEs.

In essence, we have found that elimination of IDEs has remarkably little impact on the collective protective potential of polyclonal CD8-T<sub>M</sub> cells. This gives reasonable evidence to predict that CD8 T-cell-based immunotherapy of CMV infection will be fairly robust toward even major antigenic differences between donor and recipient CMV variants.

## MATERIALS AND METHODS

**Generation of virus mutants.** Recombinant plasmids were constructed according to established procedures, and enzyme reactions were performed as recommended by the manufacturers. Throughout, the fidelity of PCR-based cloning steps was verified by sequencing (GENterprise, Mainz, Germany).

(i) **Shuttle plasmid for mutagenesis.** pST76K-m164Ala was constructed to introduce the point mutation Ala (codon GCC) in place of Ile (codon ATC) at the C-terminal MHC-I anchor residue position of the m164 peptide.

Plasmid pDrive-m164 was generated as a first intermediate. For this, a fragment of the mCMV genome including the *m164* gene was amplified from full-length mCMV bacterial artificial chromosome (BAC) plasmid pSM3fr (61) by PCR using oligonucleotides m164BAC-for (5'-AAAAGTTAACGTTTTTATG CAGCATTCGCC-3'; HpaI site underlined) and m164BAC-rev (5'-AAAAGC ATGCAGCTGTGAGATGAACTTGGTAGTCC-3'; SphI site underlined). The 5,258-bp amplification product, encompassing mCMV *m164* and flanking sequences from map positions nucleotide (nt) 225678 to 220441 (GenBank accession no. NC\_004065, complete genome) (48), was cloned into pDrive by means of UA-based ligation (catalog no. 231122; Qiagen, Hilden, Germany).

Plasmid pBlue-m164 was generated as a second intermediate. For this, pDrive-m164 was cleaved with EcoRI, and a 5,279-bp EcoRI fragment, encompassing the m164 peptide coding sequence, was inserted into EcoRI-cleaved vector pBluescript II (Stratagene, La Jolla, CA).

The third intermediate plasmid, pBlue-m164-I265A, was constructed as follows: a 1,291-bp AgeI/NcoI fragment carrying the Ala codon GCC in place of the Ile codon ATC was generated via site-directed mutagenesis by overlap extension using PCR (19) with pBlue-m164 as template DNA and with primers m164Mut-rev (5'-CGTCCGACGCGCAGCAAGCGTTTCG-3'; nt 222376 to 222400) and

m164Ala-for (5'-GGTACTCGCGCGCCTTCTGGGCCG-3'; nt 222868 to 222,845, codon of mutated amino acid in bold type) as well as m164Ala-rev (5'-CGGCCAGAAAGGCGCGAGTACC-3'; nt 222845 to 222868, codon of mutated amino acid in bold type) and m164Mut-for (5'-CCTGACCGCGAT CTGCTGGTCCCG-3'; nt 223745 to 223721). In the subsequent fusion reaction, primers m164Mut-rev and m164Mut-for were used. PCR was performed with cyler conditions as follows: an initial step for 5 min at 95°C for activation of ProofStart *Taq* DNA polymerase (catalog no. 202205; Qiagen) was followed by 30 cycles for 45 s at 94°C, 60 s at 65°C, and 60 s at 72°C. pBlue-m164 was digested with AgeI and NcoI, and the 1,291-bp AgeI/NcoI fragment was replaced with the PCR-mutated 1,291-bp AgeI/NcoI fragment. Finally, pBlue-m164-I265A was cleaved with HpaI and SphI, and the resulting 5,244-bp HpaI/SphI fragment was ligated into the SmaI/SphI-cleaved shuttle plasmid pST76-KSR (5, 47).

(ii) **Shuttle plasmid for reverse mutation.** For construction of shuttle plasmid pST76K-m164Ile, pBlue-m164 was cleaved with HpaI and SphI, and a 5,244-bp HpaI/SphI fragment, encompassing the m164 peptide coding sequence, was ligated into the SmaI/SphI-cleaved vector pST76-KSR.

(iii) **BAC mutagenesis.** Mutagenesis of full-length mCMV BAC plasmid pSM3fr (63) was performed in *Escherichia coli* strain DH10B (Invitrogen, Karlsruhe, Germany) by using a two-step replacement method (35, 43) with modifications described previously by Wagner et al. (63) and Borst et al. (4, 5). Shuttle plasmid pST76K-m164Ala was used to generate BAC plasmid C3X-m164Ala, which contains the mutated codon GCC corresponding to the amino acid point mutation I265A in the m164 peptide sequence. For construction of the double mutant C3X-IE1Ala+m164Ala with C-terminal MHC anchor residue mutations in antigenic peptides IE1 and m164, shuttle plasmid pST76K-IE1Ala (58) was transformed in *E. coli* DH10B containing BAC plasmid C3X-m164Ala. To restore Ile in position 265 of m164 and Leu in position 176 of IE1, shuttle plasmid pST76K-m164Ile encompassing the Ile codon ATC and shuttle plasmid pST76K-IE1Leu (58) encompassing the Leu codon CTA were both used for recombination resulting in BAC plasmid C3X-IE1Leu+m164Ile. Finally, shuttle plasmid pST76K-m164Ile was transformed in *E. coli* DH10B containing BAC plasmid C3X-m164Ala to generate revertant BAC plasmid C3X-m164Ile.

(iv) **Test for integrity and sequence analysis of recombinant mCMV BAC plasmids.** BAC plasmid DNA was isolated from small-scale cultures and purified (58). The overall integrity of the recombinant BAC plasmids was tested by standard methods of restriction enzyme cleavage, agarose (0.7%, wt/vol) gel electrophoresis, and ethidium bromide staining. The point mutations in recombinant mCMV BAC plasmids C3X-m164Ala, C3X-m164Ile, C3X-IE1Ala+m164Ala, and C3X-IE1Leu+m164Ile were verified by sequencing (GENterprise, Mainz, Germany).

(v) **Reconstitution of BAC-derived recombinant viruses.** Purified DNA of the respective BAC plasmids (see above) was transfected into mouse embryo fibroblasts (MEF) by using PolyFect transfection reagent (catalog no. 301107; Qiagen). To eliminate BAC-vector sequences that could attenuate viruses for growth in vivo (63), BAC-derived viruses were subjected to five rounds of passaging in MEF cultures. To verify the absence of BAC vector sequences from the recombinant mCMV genomes, PCRs and subsequent analyses were performed as described previously (15, 58). Verified BAC vector-free virus clones were used to prepare high-titer stocks of sucrose gradient-purified viruses (31, 46) mCMV-m164-I265A, mCMV-m164-A265I, mCMV-IE1-L176A+m164-I265A (abbreviated as mCMV-ΔIDE), and mCMV-IE1-A176L+m164-A265I (abbreviated as mCMV-revΔIDE). Other viruses used in this study include mCMV-IE1-L176A and mCMV-IE1-A176L (58), mCMV-Δm04+m06+m152 (62), as well as the two mCMV WT viruses mCMV-WT.Smith (ATCC VR-194; reaccessioned as VR-1399) and BAC-derived mCMV MW97.01 (63), here abbreviated as mCMV-WT.BAC.

**Procedures of infection.** (i) **Infection of mice.** Subcutaneous, intraplantar infection of adult, female BALB/cJ mice (haplotype *H-2<sup>d</sup>*) was performed at the left hind footpad with 10<sup>5</sup> PFU of the viruses indicated. For the testing of viral fitness in vivo and for adoptive T-cell transfers, 8- to 9-week-old weight-matched mice were immunocompromised by a hematopoietic total-body  $\gamma$ -irradiation with the single doses indicated below, delivered by a <sup>137</sup>Cs  $\gamma$ -ray source. Infection was performed ~2 h later. Mice were bred and housed under specific-pathogen-free conditions at the Central Laboratory Animal Facility of the Johannes Gutenberg University, Mainz. Animal experiments were approved according to German federal law, permission numbers 177-07/021-28 and 177-07/04/051-62.

(ii) **Infection of cells.** BALB/c MEF were isolated as described previously (46) and were centrifugally infected with 0.2 PFU per cell, which results in an effective multiplicity of infection (MOI) of 4 (31, 46). For use as stimulator cells in the enzyme-linked immunospot (ELISPOT) assay (see below), infected MEF were incubated for another 60 min.

**Western blot analysis of protein expression kinetics.** The expression of authentic and mutated IE1 and m164 proteins was monitored for the time course of infection of MEF in cell culture. At the indicated time points, the total protein content of infected MEF was isolated from cell lysates for subsequent Western blot analysis. In brief, infected MEF monolayers grown on 10-cm-diameter tissue culture dishes containing  $\sim 2.5 \times 10^6$  cells per dish were washed twice with ice-cold phosphate-buffered saline (PBS). Cells were scraped off, sedimented, and lysed with 200  $\mu$ l of lysis buffer (50 mM HEPES, pH 7.5, 0.2 M NaCl, 1% [vol/vol] Triton X-100, 0.4 mM EDTA, 1.5 mM  $MgCl_2$ , 0.5 mM dithiothreitol, and protease inhibitor cocktail tablets [1:25; catalog no. 1 697 498; Roche Diagnostics, Mannheim, Germany]). The cell lysates were centrifuged for 10 min at  $20,000 \times g$  at 4°C. Protein concentrations of the supernatants were determined using a bicinchoninic acid protein assay kit (catalog no. 23225; Pierce, Rockford, IL). Aliquots containing 30  $\mu$ g of protein were prepared in sodium dodecyl sulfate sample buffer and were subjected to 12.5% polyacrylamide-sodium dodecyl sulfate gel electrophoresis. The separated proteins were transferred onto polyvinylidene fluoride membranes (Immobilon-P, catalog no. IPVH0010; Millipore, Bedford, MA) by semidry blotting. For prevention of nonspecific binding, the membranes were saturated for 1 h with 5% (wt/vol) milk powder ([MP] catalog no. T145.3; Roth, Karlsruhe, Germany) in PBS-Triton (0.1% Triton X-100 in PBS, pH 7.2). Membranes were then incubated overnight at 4°C with the respective primary antibodies diluted in PBS-Triton supplemented with 1% MP. Specifically, monoclonal antibody CROMA 101 (kindly provided by S. Jonjic, Rijeka, Croatia) and polyclonal affinity-purified rabbit antibodies (21) were used for the detection of the proteins IE1-pp89/76 and m164-gp36.5, respectively. After five washes with PBS-Triton-1% MP, the membranes were incubated for 1 h at room temperature with horseradish peroxidase-conjugated rabbit anti-mouse and swine anti-rabbit antibodies (1:10,000 in PBS-Triton-1% MP; catalog no. P0260 and P0217; DAKO, Glostrup, Denmark) as second antibody, respectively. Membranes were washed five times in PBS-Triton, and bound antibodies were visualized by enhanced chemiluminescence using an ECL Plus Western blotting detection system (catalog no. RPN2132; Amersham Biosciences, Little Chalfont, United Kingdom) and Lumi-Film (catalog no. 11666657001; Roche, Diagnostics, Mannheim, Germany). Finally, the polyvinylidene fluoride membranes were stained with Coomassie blue R-250 to verify equal protein loading of the lanes.

**Immunofluorescence analysis of protein localization.** The intracellular localization of authentic and mutated IE1 and m164 proteins was visualized by confocal laser scanning immunofluorescence analysis. In brief,  $\sim 7 \times 10^4$  MEF per acetone-cleaned glass coverslip were grown for 24 h in 24-well tissue culture plates. The cells were then infected at an MOI of 4 with the respective recombinant viruses. Six hours after infection, cells were washed with PBS and then fixed for 20 min at room temperature with 4% (wt/vol) paraformaldehyde in PBS supplemented with 4% (wt/vol) sucrose. After fixation, cells were preincubated with blocking-buffer (PBS supplemented with 0.3% [vol/vol] Triton X-100 and 15% [vol/vol] fetal calf serum) for 30 min at room temperature. After this, 50  $\mu$ l of blocking buffer containing IE1- or m164-specific primary antibody (see above) was added to each coverslip, followed by an overnight incubation in a humidity chamber. After five washes with PBS, each coverslip was incubated for 1 h with the appropriate secondary antibody diluted in blocking buffer. Specifically, Alexa Fluor 488-conjugated goat anti-mouse antibody (catalog no. A11001; Molecular Probes, Eugene, OR) and Alexa Fluor 546-conjugated goat anti-rabbit antibody (catalog no. A11010; Molecular probes) were used to label IE1 protein in green and m164 protein in red, respectively. This and all subsequent incubations were performed at room temperature in the dark. After five additional washes with PBS, cell nuclei were stained by incubation of the coverslips for 5 min with the DNA-binding, blue fluorescing dye Hoechst 33342 (catalog no. H-3570; Molecular Probes) dissolved in PBS. Finally, cells were washed three times in PBS, and the coverslips were mounted in GelMount aqueous mounting medium (catalog no. G0918; Sigma-Aldrich, Steinheim, Germany) for storage at 4°C in the dark. Immunofluorescence was examined using a Zeiss laser scanning microscope (LSM 510).

**Comparison of the replicative fitness of viruses in tissues of the immunocompromised host.** The *in vivo* replicative potential of viruses was determined by establishing virus growth curves for host tissues in the absence of immune control. Specifically, BALB/c mice were immunodepleted by a 7-Gy total-body  $\gamma$ -irradiation and were infected (see above) with viruses of interest. At defined time points after the intraplantar infection, virus replication in spleen and lungs was assessed by quantification of infectious virus in the respective organ homogenates by using a virus plaque assay (PFU assay) on subconfluent second-passage MEF monolayers with the technique of centrifugal enhancement of infectivity, as described in greater detail elsewhere (46). Growth curves were established on the basis of four mice tested individually

per time point. The significance of growth differences between two viruses compared in the assay is evaluated by using distribution-free Wilcoxon-Mann-Whitney (rank sum) statistics (see below).

**Antigenic peptides and epitope-specific cytolytic T lymphocytes (CTL) and CTL lines (CTLL).** A list of the currently known mCMV-specific *H-2<sup>d</sup>* class I (*K<sup>d</sup>*, *D<sup>d</sup>*, and *L<sup>d</sup>*)-restricted antigenic peptides has been published previously (22, 49).

For the identification of new antigenic peptides, prediction algorithms provided by databases SYFPEITHI (<http://www.uni-tuebingen.de/uni/kxi/>; last accessed 13 March 2008) and RANKPEP (<http://bio.dfci.harvard.edu/Tools/rankpep.html>; last accessed 13 March 2008) were used. Custom peptide synthesis to a purity of >80% was performed by Jerini Peptide Technologies (Berlin, Germany). IE1 and m164 epitope-specific polyclonal CTLL were generated from memory spleen cells of BALB/c mice at >3 months after infection with mCMV-WT.Smith essentially as described previously (27, 46). After five rounds of stimulation with the optimized concentration ( $10^{-9}$  M) of synthetic peptides IE1 (YPHFMPNTL) and m164 (AGPPRYSRI), the CTL still expressed CD8 and were epitope specific but still polyclonal, with a broad T-cell receptor (TCR) V $\beta$  chain usage in the case of IE1-CTLL (3, 44) and a preferential but not exclusive usage of V $\beta$ 14 in the case of m164-CTLL (R. Holtappels, unpublished data).

**ELISPOT assay.** A gamma interferon (IFN- $\gamma$ )-based ELISPOT assay was used to detect sensitization of CD8 T cells by MHC-I-presented synthetic or naturally processed peptides resulting in secretion of IFN- $\gamma$ . For measuring frequencies of responding CD8 T cells, optimized epitope presentation was achieved by using P815 mastocytoma cells as stimulator cells exogenously loaded for  $\sim 1$  h with synthetic peptides at saturating concentrations. For the determination of functional avidities, the loading concentrations of peptides were graded in log<sub>10</sub> steps as indicated in the figures, followed by washing to remove unbound peptide. The presentation of naturally processed peptides was tested with MEF as stimulator cells infected with the viruses of interest. The assay was performed as described in greater detail previously (44) with  $10^5$  stimulator cells per assay culture and with graded numbers of effector cells, CTLL or *ex vivo* CD8-T<sub>M</sub> cells, seeded in triplicates. CD8-T<sub>M</sub> cells derived from the spleen were purified by two-column positive immunomagnetic cell sorting (44). After 18 h of cocultivation, plates were developed, and spots were counted. Frequencies of IFN- $\gamma$ -secreting, spot-forming cells and the corresponding 95% confidence intervals were calculated by intercept-free linear regression analysis as described previously (44).

**Viral genome-wide ORF library screening for monitoring of specificity repertoires.** For monitoring of the viral specificity repertoires of primed *ex vivo* CD8 T-cell populations, the recently developed mCMV open reading frame (ORF) library spanning the whole mCMV genome (41) was employed with minor modifications. In brief, simian virus 40 (SV40)-transformed BALB/c fibroblasts (kindly provided by D. Johnson, Oregon Health and Science University, Portland, OR) were plated at a density of 6,000 cells per well in 96-well flat-bottomed microwell plates. On the following day, cells in each well were transfected with  $\sim 30$   $\mu$ l of a mixture containing 10  $\mu$ l of ORF plasmid DNA (250 ng) and 0.75  $\mu$ l of FuGENE 6 (catalog no. 11 814 443 001; Roche) diluted in OptiMEM I (catalog no. 51985-026; Gibco). Each transfection was carried out in duplicate microcultures. Two days later,  $1 \times 10^6$  erythrocyte-depleted splenocytes from mCMV-primed mice were added per transfection microculture and incubated for 6 h at 37°C in the presence of brefeldin A (BD GolgiPlug; final concentration, 1:1,000) (catalog no. 555029; BD Biosciences Pharmingen) to block secretion of IFN- $\gamma$ . For known epitope specificities, control microcultures of the splenocytes seeded at a density of  $2 \times 10^6$  cells per well in a 96-well round-bottom microwell plate were restimulated with the respective synthetic peptides added in the optimized final concentration of  $5 \times 10^{-7}$  M and were incubated in the presence of brefeldin A, accordingly.

For the intracellular cytokine assay, effector cells derived from each pair of transfection cultures, that is, cultures representing the same ORF, were combined and transferred into a microculture of round-bottomed 96-well plates. The stimulated effector cells from both the transfection cultures and the peptide control cultures were cell surface stained with phycoerythrin (PE)-Cy5-labeled anti-mouse CD8a (Ly-2) monoclonal antibody (clone 53-6.7; catalog no. 553034; BD Biosciences Pharmingen), fixed and permeabilized with BD Cytotfix/Cytoperm (catalog no. 554722; BD Biosciences Pharmingen), and stained for intracellular IFN- $\gamma$  with fluorescein isothiocyanate-labeled anti-mouse IFN- $\gamma$  monoclonal antibody (clone XMG1.2; catalog no. 554411; BD Biosciences Pharmingen) diluted in BD Perm/Wash Buffer (catalog no. 554723; BD Biosciences Pharmingen). Electronic gates were set on lymphocytes and on positive PE-Cy5 fluorescence to restrict the analysis of IFN- $\gamma$  expression to CD8 T lymphocytes. The cytofluorometric measurements were performed with a FACSort instrument using CellQuest Pro software for data processing (Becton Dickinson).

**Adoptive cell transfer and quantitation of infection in host tissues.** Donors of CD8-T<sub>M</sub> cells for adoptive cell transfers were female BALB/c mice infected at the age of 8 to 10 weeks with the viruses under investigation. Three months after infection at the earliest, splenocytes from at least three mice per group were pooled, and CD8 T cells were isolated by positive immunomagnetic cell sorting (44). Recipients of the adoptive cell transfer were 8- to 9-week-old female BALB/c mice immunocompromised by  $\gamma$ -irradiation with a single dose of 6.5 Gy. Graded numbers of CD8 T cells derived from the mCMV-primed donor mice or from age-matched naive control mice were transferred 4 h later by intravenous infusion. Subcutaneous, intraplantar infection was performed ~2 h after cell transfer with 10<sup>5</sup> PFU of mCMV-WT.BAC or recombinant mCMVs. Organ infection was monitored on day 11 after cell transfer. Infectious virus present in the spleens and lungs was quantitated in organ homogenates by the virus plaque assay on MEF. Infection of the liver was assessed from the number of infected cells detected in liver tissue sections by IE1-pp89/76-specific immunohistochemistry using the peroxidase-diaminobenzidine-nickel method for black staining of infected cell nuclei (27, 46).

**Statistical analysis.** The statistical significance of differences in virus titers was evaluated by using distribution-free Wilcoxon-Mann-Whitney (rank sum) statistics. An online calculator is provided on the website <http://elegans.swmed.edu/~leon/stats/utest.html> (last accessed 13 March 2008; Ivo Dinov, Statistics Online Computational Resources, UCLA Statistics, Los Angeles, CA). Virus titers in two experimental groups differ significantly if the *P* value (two-tailed test) is <0.05.

## RESULTS

**Approach for deleting IDEs.** In the BALB/c mouse model of CMV infection, the CD8-T<sub>M</sub> cell specificity repertoire is largely focused on two IDEs of mCMV, namely the IE1 (pp89/76)-derived antigenic peptide 168-YPHFMPTNL-176 and the m164 (gp36.5)-derived antigenic peptide 257-AGPPRYSRI-265 presented by the MHC-I molecules L<sup>d</sup> and D<sup>d</sup>, respectively. Using BAC mutagenesis (7), we constructed virus mCMV- $\Delta$ IDE, in which both immunodominant epitopes are functionally deleted by replacing the C-terminal MHC-I anchor residue of each peptide with Ala (Fig. 1). Both mutations were reversed in revertant virus mCMV-rev $\Delta$ IDE by replacing the Ala codons with the codons for the original amino acids. Subsequently, mutant and revertant were analyzed for their functional integrity. The epitope mutations had no adverse effects on the expression of the corresponding proteins (Fig. 2A). Specifically, the kinetics of expression and the molecular masses were unaltered, and in the case of IE1, posttranslational modification of the 89-kDa form to the 76-kDa form was not affected. Likewise, nuclear localization of IE1 as well as cytoplasmic localization of m164 was not altered by the mutations (Fig. 2B). Furthermore, the two viruses replicate with the same kinetics and to the same infectivity titers in spleen and lungs of immunocompromised recipients (Fig. 2C). These data provide reasonable evidence to conclude that the two epitope mutations do not significantly affect viral replicative fitness in the absence of immune control.

**Verification of the intended immunological phenotype of the epitope mutations.** In previous work, the strategy of abrogating antigenicity and immunogenicity by an Ala point mutation of the C-terminal MHC-I anchor residue of an antigenic peptide was successfully applied for the single-IDE deletion mutant mCMV-IE1-L176A (58). When tested as a synthetic peptide for exogenous loading, the C-terminal Ala variant YPHFMPTNA of the IE1 peptide was found to bind to the L<sup>d</sup> molecule only with very low affinity (52, 54, 58), and in vivo the corresponding mutant virus failed to prime CD8 T cells recognizing the IE1 peptide or its C-terminal Ala variant (58). To confirm

the intended “lack of antigenicity phenotype” of the dual-IDE deletion mutant mCMV- $\Delta$ IDE, the absence and presence of peptide presentation in cells infected with the mutant and the revertant, respectively, are documented (Fig. 3). Epitope-specific but still polyclonal IE1-CTLL and m164-CTLL, representing a range of TCR affinities, served as probes for detecting presented peptides. While basically all cells of the two CTLL recognized their cognate epitopes presented by MEF infected with the immune evasion gene deletion mutant mCMV- $\Delta$ m04+m06+m152 (62; for a review, see reference 49), immunoevasins expressed in MEF infected with mCMV-WT.BAC markedly reduced the presentation. Nevertheless, in both CTLL ~20% of the cells were of a functional avidity sufficient to detect presented peptide even though the viral immune evasion mechanisms were operative. Upon testing a complete set of all possible combinations of deletion and expression of the two IDEs, IE1-CTLL and m164-CTLL selectively failed to detect the IE1 and m164 epitopes on MEF infected with viruses carrying the L176A and the I265A mutations, respectively. Specifically, as intended by the mutational design, both CTLL failed to recognize MEF infected with mCMV- $\Delta$ IDE but recognized MEF infected with mCMV-rev $\Delta$ IDE.

**Ex vivo CD8-T<sub>M</sub> cells recognize infected cells in the absence of IDEs IE1 and m164.** Polyclonal populations of CD8-T<sub>M</sub> cells primed by infection of BALB/c mice with mCMV-WT.Smith were originally shown to display a specificity repertoire focused on IDEs IE1 and m164 (27). This previous finding was essentially reproduced here for the priming with mCMV-rev $\Delta$ IDE by determining the frequencies of CD8-T<sub>M</sub> cells responding to exogenously loaded synthetic peptides corresponding to all currently known *H-2<sup>d</sup>*-restricted epitopes of mCMV (Fig. 4A). A minimum estimate for the total number of CD8-T<sub>M</sub> cells specific for known and unknown epitopes of mCMV was obtained with MEF infected with mCMV- $\Delta$ m04+m06+m152, in which epitope presentation after endogenous processing is not hindered by immunoevasins (Fig. 4B). The frequency of ~3% compared with a cumulative frequency of ~1.5% measured for the known epitopes with the very same CD8-T<sub>M</sub> cell population indicated for the first time that a significant proportion of mCMV-specific CD8-T<sub>M</sub> cells recognize mCMV epitopes not covered by the known antigenic peptides. Expression of immunoevasins by mCMV-WT.BAC reduced the number of MHC-peptide complexes at the cell surface so that only one-third of the mCMV-specific CD8-T<sub>M</sub> cells, most likely those with high functional avidity, were still capable of recognizing the infected cells. Predictably, the same result was obtained with cells infected with mCMV-rev $\Delta$ IDE. Surprisingly, absence of the two IDEs in cells infected with mCMV- $\Delta$ IDE did not, however, significantly reduce the frequency of responding cells. This finding indicated that CD8-T<sub>M</sub> cells specific for the two IDEs are dispensable for the recognition of infected cells. This is essentially new information in CMV immunology.

In the second part of the experiment, we investigated the reciprocal situation of CD8-T<sub>M</sub>-cell donors being primed with mCMV- $\Delta$ IDE (Fig. 4C and D). In accordance with successful epitope deletions, mCMV- $\Delta$ IDE did not prime for the generation of IE1- and m164 epitope-specific CD8-T<sub>M</sub> cells. Unexpectedly, however, the response to the currently known subdominant epitopes did not profit from the absence of the two IDEs (Fig. 4C). That the IDE deletion is not fully compensated

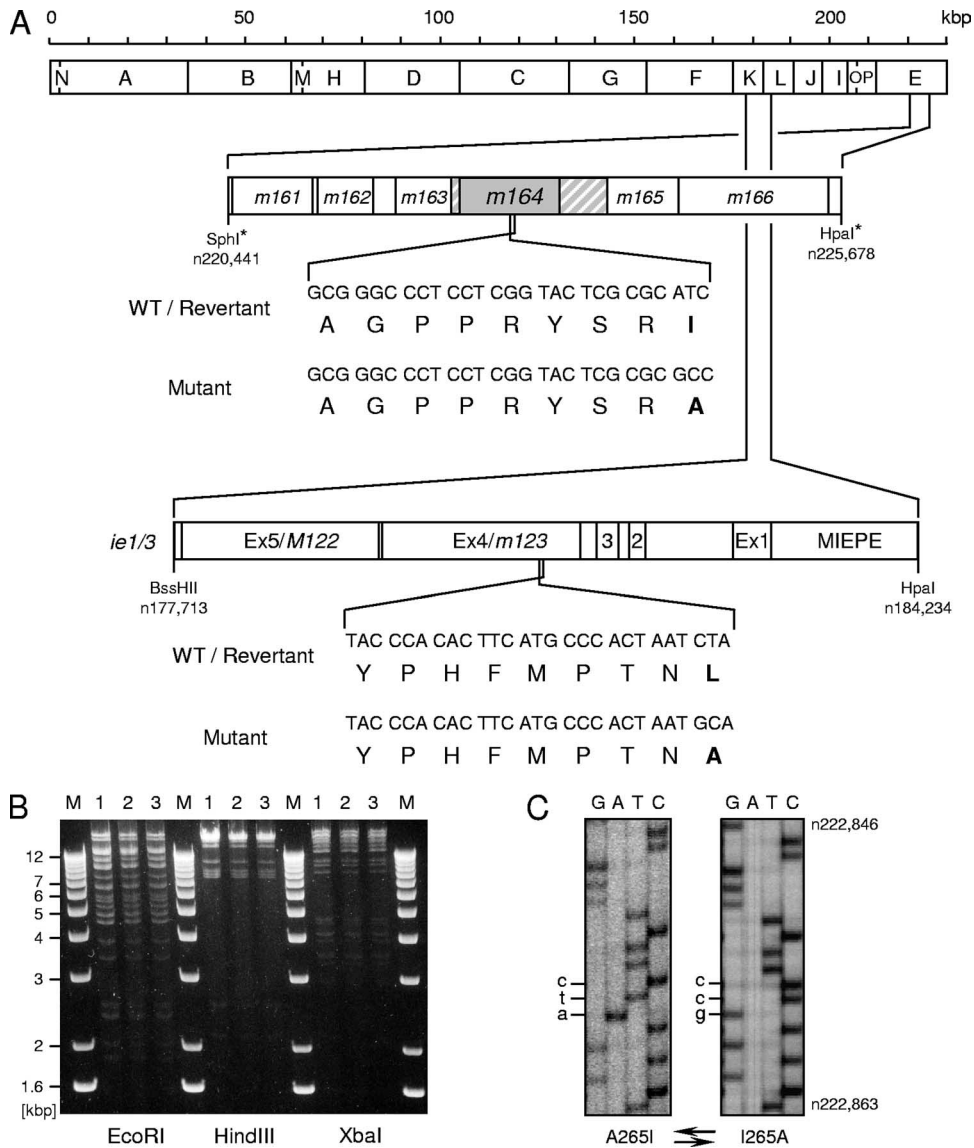


FIG. 1. Construction and verification of recombinant viruses. (A) Maps, drawn to scale, illustrating the mutagenesis strategy. The HindIII physical map of the mCMV Smith strain genome (mCMV-WT.Smith) is shown at the top. The genomic regions encompassing genes *m161* through *m166* (SphI-HpaI fragment; \*, restriction sites SphI and HpaI inserted by PCR) and the *ie1-ie3* transcription unit (BssHII-HpaI fragment) are expanded to reveal the locations of the coding sequences for the authentic antigenic peptides *m164* and *IE1* in mCMV-WT and revertant virus mCMV-revΔIDE. The gray-shaded area represents ORF *m164*, with striated portions showing the overlap with neighboring ORFs, based on Rawlinson et al. (48). By means of site-directed BAC mutagenesis, the C-terminal MHC-I anchor residues Ile and Leu of the antigenic peptides *m164* and *IE1*, respectively, were replaced with Ala. Amino acids and the corresponding codons are specified. (B) Structural analysis of BAC plasmids. Purified DNA of BAC plasmids pSM3fr (lanes 1), C3X-IE1Ala-*m164*Ala (lanes 2), and C3X-IE1Leu-*m164*Ile (lanes 3) was subjected to cleavage by EcoRI, HindIII, and XbaI. Fragments were analyzed by agarose gel electrophoresis and staining with ethidium bromide. Lanes M show the size markers. (C) Sequence analysis of mutated BAC plasmids. The fidelity of the reverted and the mutated *m164* sequences is shown between nt 222846 and 222863 for the BAC plasmids C3X-IE1Leu-*m164*Ile (revertant A265I) and C3X-IE1Ala-*m164*Ala (mutant I265A). The fidelity of the reverted and mutated *ie1* sequences has been documented previously (58).

for by other epitopes is indicated by a small but statistically significant reduction in the total frequency of mCMV-specific CD8-T<sub>M</sub> cells detected in the absence of immune evasion genes (compare Fig. 4D and B) (there is no overlap in the 95% confidence intervals). As expected from the absence of IDE-specific cells in the CD8-T<sub>M</sub>-cell population, the recognition of target cells infected with mCMV-WT.BAC, mCMV-revΔIDE, and mCMV-ΔIDE was identical within the 95% confidence

intervals (Fig. 4D). Strikingly, however, this recognition was not reduced in comparison with the CD8-T<sub>M</sub>-cell population containing IDE-specific cells (compare Fig. 4D and B).

Collectively, these data strongly suggest that presence of the two IDEs does not significantly add to the recognition of infected cells by polyclonal CD8-T<sub>M</sub> cells.

**Identification of an epitope in ORF *m145* that profits from the deletion of IDEs.** The analysis of mCMV-specific CD8-T<sub>M</sub>-

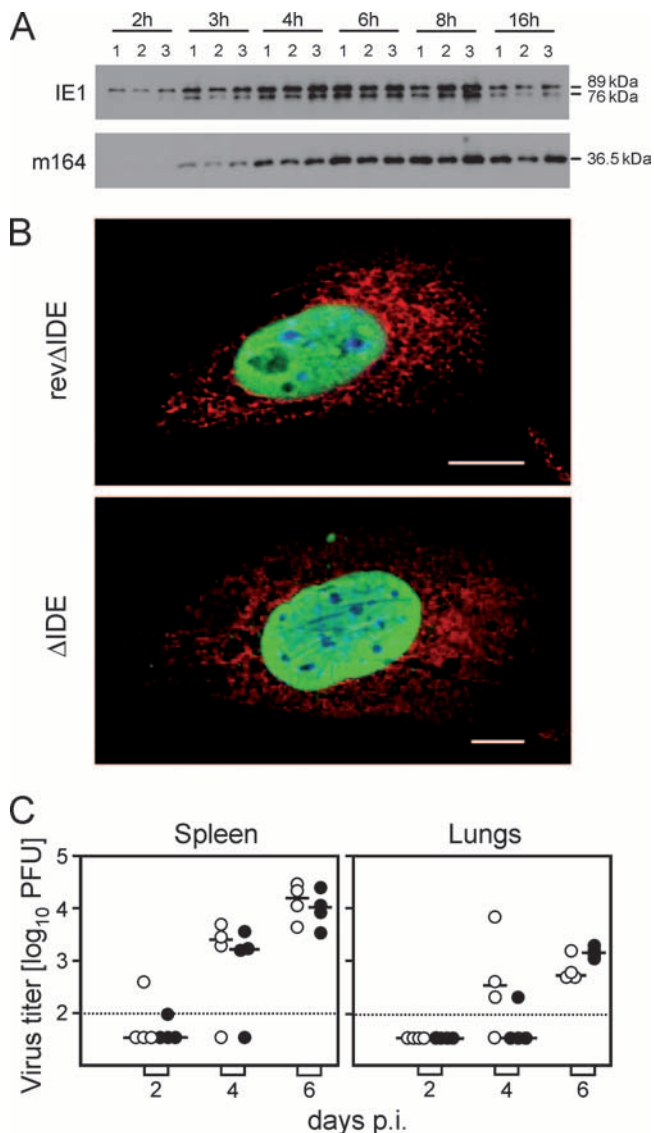


FIG. 2. Phenotypic integrity of mutant virus mCMV- $\Delta$ IDE. (A) Protein expression kinetics. Western blots showing the expression of the two IE1 protein species pp89-kDa and pp76-kDa (IE1) as well as of m164 gp36.5-kDa (m164) in MEF. Lanes 1, mCMV-WT.BAC; lanes 2, mCMV- $\Delta$ IDE; lanes 3, mCMV- $\Delta$ IDE. (B) Intracellular protein distribution. Confocal laser scanning images showing intracellular location of authentic and mutated IE1 pp89/76 (Alexa Fluor 488, green) and cytoplasmic distribution of authentic and mutated m164 gp36.5 (Alexa Fluor 546, red). DNA is stained in blue by Hoechst 33342 dye showing nuclear compartments spared by IE1.  $\Delta$ IDE, MEF infected for 6 h with mCMV- $\Delta$ IDE;  $\Delta$ IDE, MEF infected for 6 h with mCMV- $\Delta$ IDE. Scale bar, 10  $\mu$ m. (C) Viral replicative fitness in vivo. Shown are virus growth curves for the spleen and lung of immunocompromised BALB/c mice. Symbols represent virus titers (per organ) for individual mice with median values indicated. Open circles, mCMV- $\Delta$ IDE; filled circles, mCMV- $\Delta$ IDE. The dotted line represents the detection limit of the virus plaque assay. p.i., postinfection.

cell repertoires was so far restricted to the limited number of epitopes identified in their amino acid sequence (22, 49). The recognition of infected cells not expressing immunoevasins, however, has suggested the existence of a substantial propor-

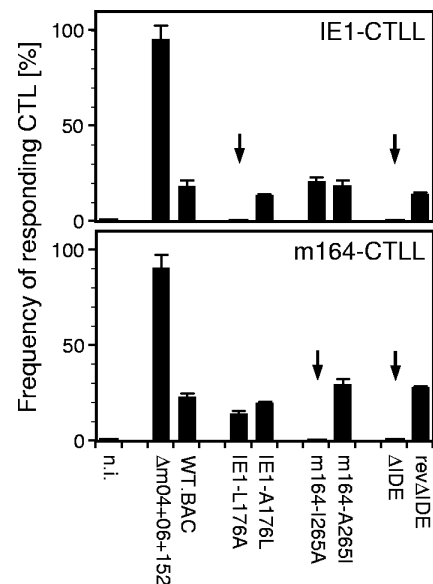


FIG. 3. Verification of the intended epitope-specific loss-of-antigenicity phenotype of mCMV- $\Delta$ IDE. MEF were infected with the panel of viruses indicated, and the presentation of peptides IE1 and m164 was monitored in an IFN- $\gamma$  secretion-based ELISPOT assay with epitope-specific but still polyclonal CTL lines IE1-CTL and m164-CTL as effector cells, respectively. Bars represent the frequencies of responding effector cells that have a functional avidity sufficient to detect presented peptide. Error bars indicate the upper limits of the 95% confidence intervals determined by intercept-free linear regression analysis. Arrows highlight the absence of detectable peptide presentation in cells infected with viruses carrying the respective single and dual mutations. n.i., uninfected MEF.

tion of CD8-T<sub>M</sub> cells recognizing unknown epitopes (Fig. 4). Possibly, previous studies may have failed to detect other IDEs. Alternatively, “conditional” IDEs may newly arise in the absence of the “constitutive” IDEs, or numerous subdominant epitopes individually eliciting low CD8-T<sub>M</sub>-cell frequencies may add up to a significant collective response.

This question was addressed by employing the recently established mCMV genome-spanning ORF library (see also Table S1 in the supplemental material) for antigenicity screening, which is based on transient transfection of target cells with ORF expression plasmids, followed by cytofluorometric detection of intracellular IFN- $\gamma$  in a test population of CD8 T cells stimulated with the library of transfectants (41). The recognition spectra were recorded for CD8-T<sub>M</sub> cells derived from BALB/c mice infected with mCMV- $\Delta$ IDE and, for comparison, with mCMV- $\Delta$ IDE (Fig. 5).

For the CD8-T<sub>M</sub>-cell population primed by mCMV- $\Delta$ IDE, the ORF library screening clearly confirmed the two IDE-encoding ORFs, *IE1* and *m164* (Fig. 5A), already known from previous studies that were based on mCMV-WT.Smith (27). Only a few other ORFs gave signals above background and with minor variance between different screening runs performed with independent CD8-T<sub>M</sub>-cell populations (unpublished data); but from the marked ORFs signals were more consistently detected. The results imply that “missing epitopes” predicted to exist based upon the recognition of infected target cells (see above) make only minor individual contributions to

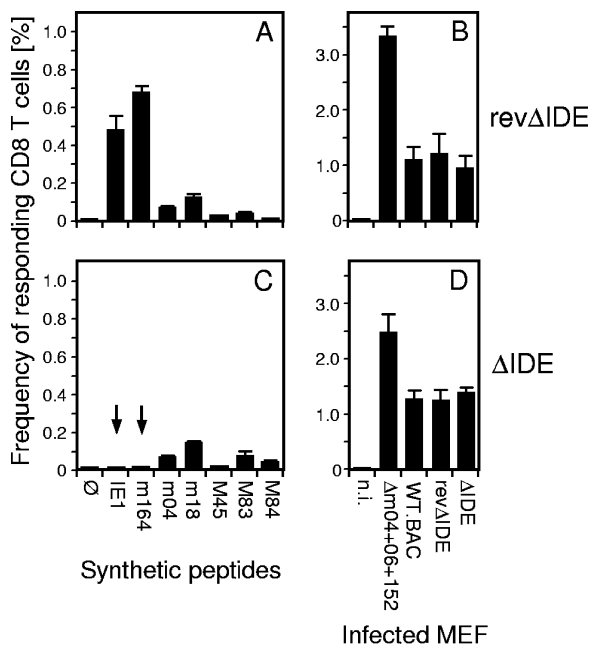


FIG. 4. Immunogenicity phenotype of mCMV-ΔIDE. BALB/c mice were infected with mCMV-revΔIDE (revΔIDE; A and B) and mCMV-ΔIDE (ΔIDE; C and D). Frequencies of CD8-T<sub>M</sub> cells present among CD8 T cells purified from the spleens (pool of three mice per group) at 3 months after infection were determined by an ELISPOT assay performed with P815 stimulator cells exogenously loaded with saturating concentrations of synthetic antigenic peptides representing the hitherto known H-2<sup>d</sup>-restricted epitopes indicated (A and C) or with MEF presenting naturally processed antigenic peptides after infection with the viruses indicated (B and D). Bars represent the frequencies of responding CD8-T<sub>M</sub> cells. For error statistics, see the legend of Fig. 3. Arrows highlight the absence of IE1- and m164-specific CD8-T<sub>M</sub> cells after infection with mCMV-ΔIDE. n.i., uninfected MEF; ∅, stimulator cells with no viral peptide added.

the CD8-T<sub>M</sub>-cell pool size, although these contributions may well cumulate to a quantitatively significant total response.

The ORF antigenicity spectrum recorded for CD8-T<sub>M</sub> cells primed with mCMV-ΔIDE revealed the loss of responses to IDEs IE1 and m164, but the absence of these two specificities caused only quite discrete rather than extensive changes in the remaining responses (Fig. 5B). An effect observed consistently, however, was the expansion of CD8-T<sub>M</sub> cells specific for ORF *m145*. We therefore set out to identify the corresponding antigenic peptide. Since it was known from our previous work that naturally processed peptides isolated from infected BALB/c MEF can select K<sup>d</sup>-restricted CTLL of unknown epitope specificity by repeated restimulation of CD8-T<sub>M</sub> cells (26), we used algorithms SYFPEITHI and RANKPEP for predicting K<sup>d</sup>-restricted peptides encoded by ORF *m145*. Peptide 451-CYYASRTKL-459 was confirmed as a CD8 T cell epitope. The m145 glycoprotein shares properties with MHC-I and is known to regulate NK cell-mediated innate immunity to mCMV by preventing the cell surface expression of the NKG2D ligand MULT-1 (30). With a similar strategy, K<sup>d</sup>-restricted peptide 207-TYWPVSDI-215 was confirmed as an epitope encoded by ORF *M105*, an ORF that is homologous to hCMV ORF *UL105* and codes for the helicase subunit of the helicase-primase complex. This specificity, however, was less

prominent in the CD8-T<sub>M</sub>-cell recognition spectra regardless of whether priming was by mCMV-revΔIDE or by mCMV-ΔIDE.

The ORF library has certainly proven its power as a valuable tool for the identification of antigenic ORFs. Nevertheless some caution is recommended with regard to interpreting the signals in quantitative terms. This is mainly because transfection efficiencies are not identical for all the different ORF expression plasmids. One also has to keep in mind that an ORF signal can represent the recognition of more than one antigenic peptide. In parallel to the ORF library screening, we therefore have measured the frequencies of epitope-specific cells by stimulating the very same CD8-T<sub>M</sub>-cell population in the same type of assay with saturating concentrations of the known antigenic peptides, including the peptides M105 and m145 newly identified here (Fig. 5, insets). For CD8-T<sub>M</sub> cells primed by mCMV-revΔIDE, this control confirmed the quantitative immunodominance of IE1 and m164, but opposite to what was suggested by the ORF library screening, IE1 prevailed over m164. M105, which was not revealed by the ORF library screening, was here represented by a detectable frequency of CD8-T<sub>M</sub> cells (Fig. 5A, inset). Like most other epitopes tested, M105 did not significantly profit from the absence of epitopes IE1 and m164 after priming with mCMV-ΔIDE, whereas a distinct advantage of m145 was confirmed (Fig. 5B, inset).

In conclusion, in the case of a complex virus with a high coding capacity, infection with a variant devoid of the IDEs of WT virus does not lead to a global alteration in the repertoire of ORFs engaged in the CD8-T<sub>M</sub>-cell response. This again is novel and surprising information in CMV immunology, made possible by the ΔIDE mutant. A discrete adaptation, however, takes place that allows expansion of CD8-T<sub>M</sub> cells specific for an otherwise subdominant epitope, which, in a way, qualifies as a conditional IDE in the sense that it becomes an IDE if constitutive IDEs are deleted.

**Deletion of constitutive IDEs has little impact on the protective efficacy of donor CD8-T<sub>M</sub> cells.** The data presented so far raised the question of whether expansion of CD8-T<sub>M</sub> cells specific for conditional IDEs, such as m145, would fully compensate for the loss of constitutive IDEs in antiviral protection. The recognition of infected cells (Fig. 4) has actually predicted this. In a first approach, we tested donor-derived CD8-T<sub>M</sub> cells primed with either mCMV-revΔIDE or mCMV-ΔIDE by adoptive transfer into immunocompromised recipients infected with mCMV-WT.BAC. In such an experimental setting, target cell infection in the recipients is a constant parameter with all epitopes being present, so that differences in the control of infection can directly be attributed to the transferred cells (Fig. 6).

For a comparison of the protective efficacies of the two CD8-T<sub>M</sub>-cell populations it is a crucial control to determine also the protective efficacy of unprimed CD8 T cells derived from CMV-naïve mice, which represent the experimental counterpart of a CMV-unexperienced donor in a D<sup>-</sup>R<sup>+</sup> constellation of clinical HSCT (see introduction). It must be recalled that an immunocompetent host controls a primary CMV infection by virtue of the presence of CMV-specific precursor CD8 T cells that get primed, expand clonally, and develop into antiviral effector cells and CD8-T<sub>M</sub> cells (51, 55). Logically,

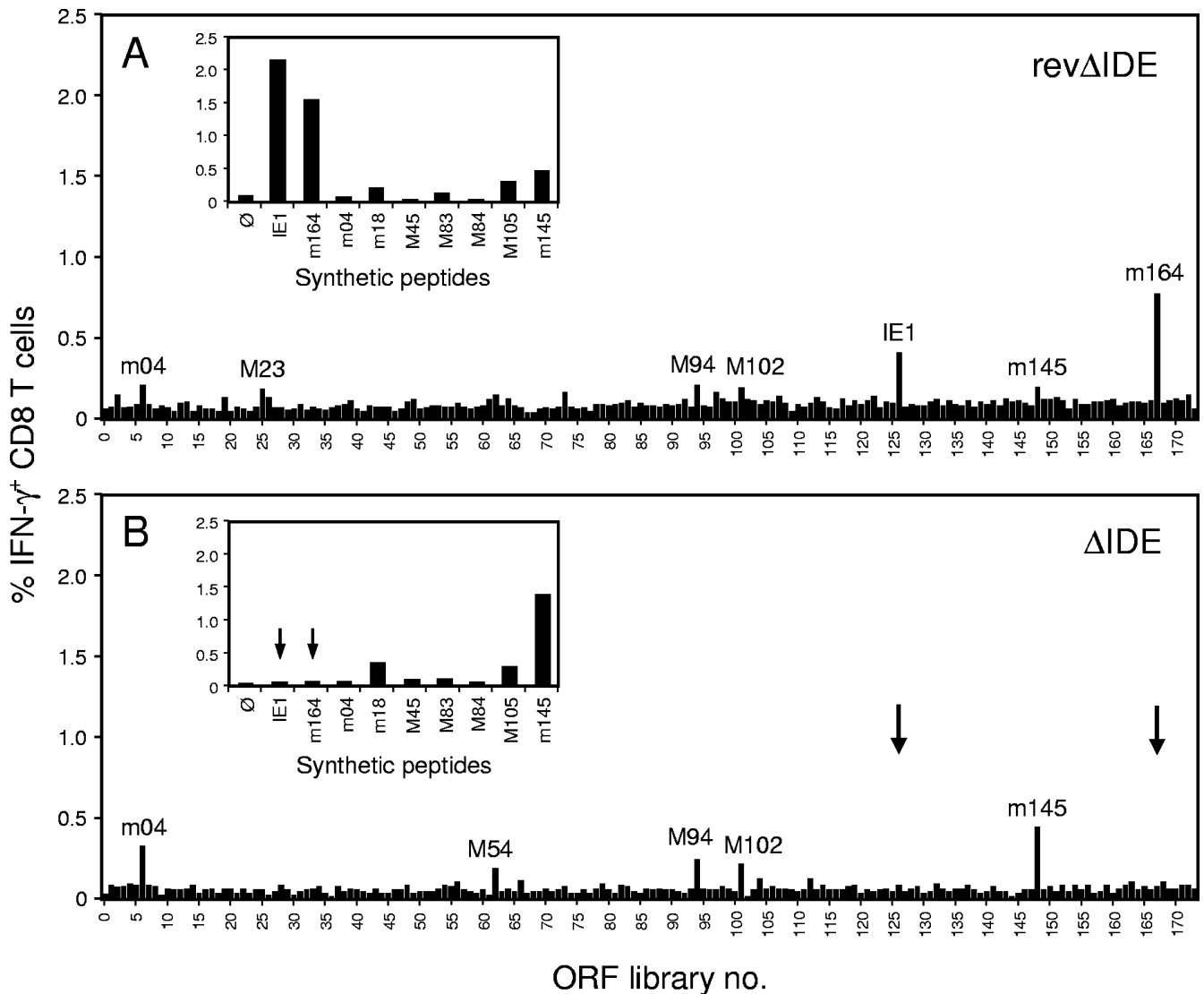


FIG. 5. Viral genome-wide ORF antigenicity spectra. The specificity repertoires of CD8-T<sub>M</sub> cells were recorded at 3 months after infection with mCMV-revΔIDE (A) or mCMVΔIDE (B) by using an ORF library of expression plasmids. For a list assigning library numbers to ORFs, see Table S1 in the supplemental material. ORFs eliciting peaks of response are indicated. Spleen cells pooled from seven donors per group were used as responder cells, and SV40-transformed BALB/c fibroblasts transiently transfected with the respective ORF expression plasmids were used as stimulator cells. Stimulation of responder cells by epitope-presenting ORF transfectants was assayed on the basis of IFN-γ synthesis by cytofluorometric intracellular cytokine staining with electronic gates set on lymphocytes and on positive PE-Cy5 (CD8a) cell surface fluorescence. For control, aliquots of the same spleen cell populations were incubated with optimized concentrations of the synthetic peptides indicated and were run in parallel in the same assay (insets). Arrows highlight the absence of IE1- and m164-specific CD8-T<sub>M</sub> cells after priming by infection with mCMV-ΔIDE. ∅, memory spleen cells with no viral peptide added.

provided that an immunocompromised host is reconstituted with a sufficiently high number of naïve CD8 T cells, infection will be controlled. The difference between pools of naïve CD8 T cells and pools of CD8-T<sub>M</sub> cells predictably lies in the “dose effectiveness” due to an expanded cell number, faster response time, and possibly also an affinity maturation (28) of CMV-specific CD8-T<sub>M</sub> cells contained in the CD8 T-cell population. A higher dose effectiveness of CD8-T<sub>M</sub> cells was indeed revealed in an immunohistological analysis of CMV infection in the liver of adoptive transfer recipients by a 100-fold lower number of cells required for the prevention of CMV hepatitis (Fig. 6A). Notably, no obvious difference in dose effectiveness

was observed, however, between CD8-T<sub>M</sub>-cell populations derived from donors primed by infection with mCMV-revΔIDE and mCMV-ΔIDE. These findings were further substantiated by a quantitative analysis of virus replication in spleen, lungs, and liver of the recipients (Fig. 6B). The impact of CMV-specific priming became particularly obvious at low cell doses, whereas absence of CD8-T<sub>M</sub> cells specific for IDEs IE1 and m164 from the donor cell population had only a minimal effect on the protection.

**Release from immunodomination is not essential for protection induced by non-IDEs.** If in the absence of constitutive IDEs an adaptation of the immune response by expansion of

Donor immune status

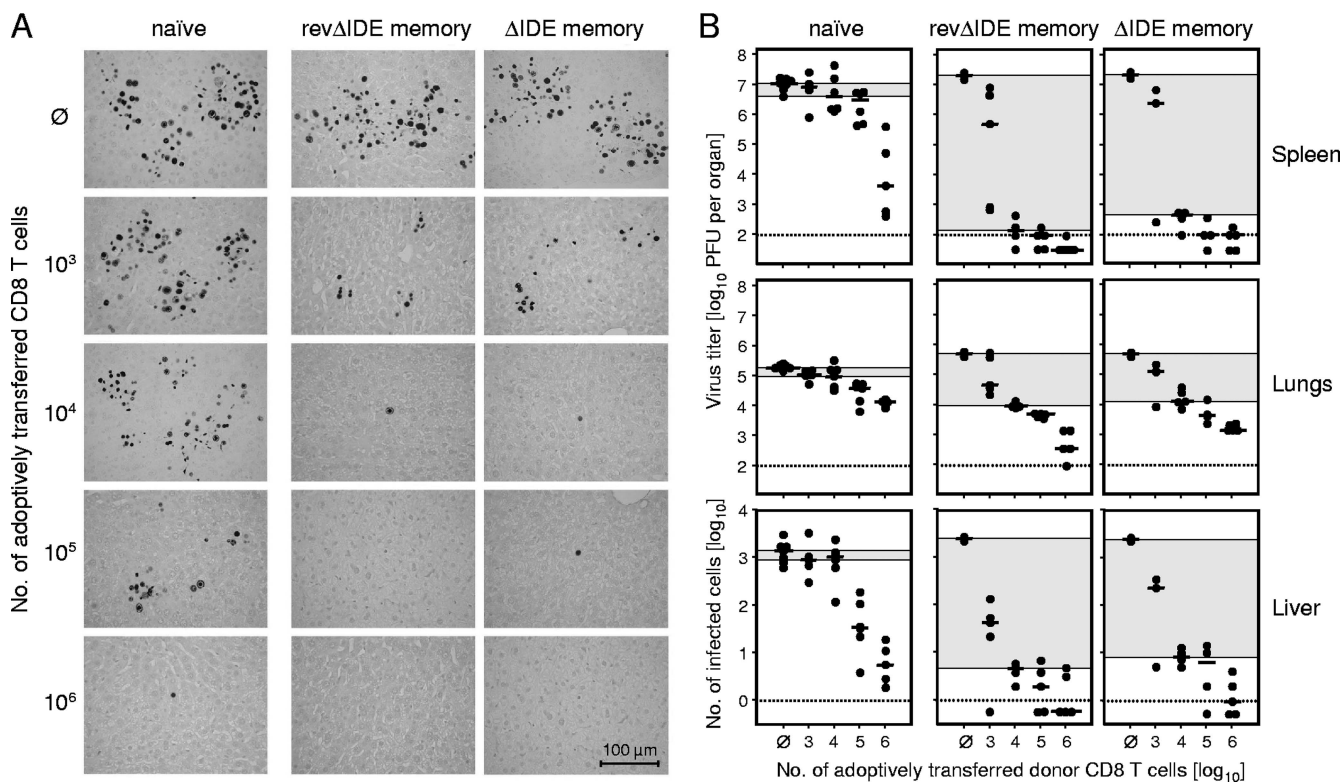


FIG. 6. Influence of donor immune status on the protective antiviral effectiveness of CD8 T cells. (A) Prevention of viral histopathology in the liver by adoptive transfer of naïve and memory CD8 T cells. The antiviral activity of CD8 T cells derived from CMV-unexperienced BALB/c donors (naïve), from donors infected 3 months earlier with mCMV-revΔIDE (revΔIDE memory), and from donors infected 3 months earlier with mCMV-ΔIDE (ΔIDE memory) was determined by adoptive transfer. Donors were from the batches of mice for which CD8-T<sub>M</sub>-cell specificity repertoires were determined in the experiment shown in Fig. 4. CD8 T cells were purified from pools of three spleens per donor group, and log<sub>10</sub>-graded numbers were transferred into immunocompromised BALB/c recipients infected with mCMV-WT.BAC. Liver infection was assessed on day 11 by immunohistochemistry specific for the intranuclear IE1 protein pp89/76. Black staining visualizes nuclei of infected liver cells. Light counterstaining was performed with hematoxylin. ∅, no cells transferred. (B) Donor cell dose-dependent reduction of virus infectivity in recipient organs. Virus replication was quantitated by measuring virus titers in homogenates of spleen and lungs and by counting of infected cells (IE1 positive, black-stained cell nuclei) in representative 10-mm<sup>2</sup> sections of liver tissue. Filled circles represent data for individual recipients with the median values marked. The dotted line indicates the detection limit of the respective assay. Antiviral protection by low doses of CD8 T cells (median values in the therapy groups with 10<sup>4</sup> CD8 T cells compared with the median values in the no-transfer control groups) is highlighted by gray shading. ∅, no cells transferred.

CD8-T<sub>M</sub> cells specific for conditional IDEs is critical for protection, CD8-T<sub>M</sub> cells specific for non-IDEs but primed under the immunodominating influence of IDEs should be the least protective. This can be tested by using recipients infected with mCMV-ΔIDE and comparing the protective function of CD8-T<sub>M</sub> cells derived from mCMV-revΔIDE-primed donors, in which immunodomination of non-IDEs by IDEs can occur, with the protective function of CD8-T<sub>M</sub> cells derived from mCMV-ΔIDE-primed donors, in which CD8-T<sub>M</sub> cells specific for non-IDEs can develop without restraint. Since IDEs are not expressed in the ΔIDE-infected recipients, IDE-specific CD8-T<sub>M</sub> cells should play no role in these recipients. It is important that control experiments with IDE-specific CTL (R. Holtappels, unpublished data) and, in the case of IE1, also with TCR-sorted polyclonal CD8-T<sub>M</sub> cells (3), have not revealed any protection of recipients infected with mCMV-ΔIDE and with the IE1 epitope deletion mutant mCMV-IE1-L176A, respectively. These findings exclude any relevant contribution

of a putative cross-recognition of other viral epitopes by IDE-specific cells due to TCR degeneracy.

Figure 7A illustrates the experimental concept of a crisscross adoptive transfer experiment in which donors were primed with mCMV-revΔIDE and mCMV-ΔIDE and in which recipients were infected accordingly with either virus. With regard to the protection against mCMV-revΔIDE that expresses all epitopes (Fig. 7B, upper panels), this experiment essentially reproduced the data obtained for the protection against mCMV-WT.BAC (recall Fig. 6) in that a CD8-T<sub>M</sub>-cell population primed with mCMV-revΔIDE was slightly more efficient in spleen and lungs, with statistical significance at 10<sup>4</sup> cells transferred (*P* = 0.024, a1 versus b1 for the spleen; *P* = 0.024, a2 versus b2 for the lungs), but not in the liver (*P* = 0.262, a3 versus b3) (Fig. 7B). Contrary to all predictions, however, protection against mCMV-ΔIDE (Fig. 7B, lower panels) was essentially the same for CD8-T<sub>M</sub> cells primed with mCMV-revΔIDE and those primed with mCMV-ΔIDE (*P* = 0.240, c1

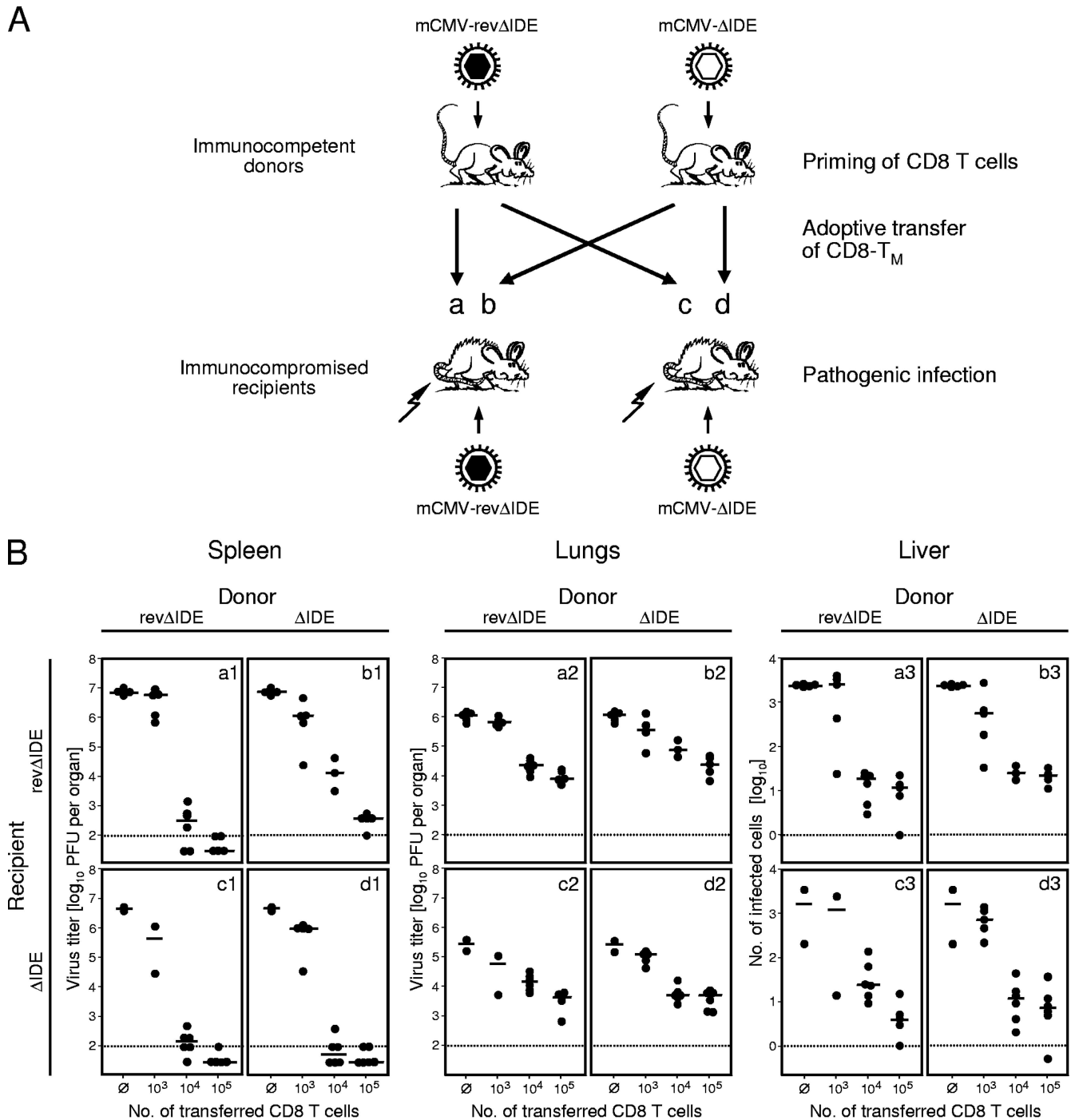


FIG. 7. Impact of an antigenicity mismatch between donor virus and recipient virus on antiviral protection mediated by CD8-T<sub>M</sub> cells. (A) Illustration of the experimental strategy of crisscross adoptive transfer. (B) Experimental results. BALB/c donors were primed by infection with mCMV-revΔIDE and mCMV-ΔIDE, and after 6 months CD8 T cells were purified from pools of three spleens per donor group. Groups of immunocompromised BALB/c recipients were infected likewise with the two viruses. Protective antiviral effectiveness of donor CD8 T cells in the spleen, lungs, and liver of the recipients was tested by adoptive transfer of log<sub>10</sub>-graded cell numbers in a crisscross scheme leading to the matching donor-recipient combinations revΔIDE-revΔIDE (a1 to a3) and ΔIDE-ΔIDE (d1 to d3) as well as to the mismatching donor-recipient combinations ΔIDE-revΔIDE (b1 to b3) and revΔIDE-ΔIDE (c1 to c3). Virus replication was quantitated on day 11 by measuring virus titers in homogenates of spleen and lungs and by counting the number of infected cells (IE1-positive, black-stained cell nuclei) in representative 10-mm<sup>2</sup> sections of liver tissue. Filled circles represent data for individual recipients, with the median values marked. The dotted line indicates the detection limit of the respective assay. ∅, no cells transferred.

versus d1 for the spleen;  $P = 0.065$ , c2 versus d2 for the lungs, and  $P = 0.093$ , c3 versus d3 for the liver, all at 10<sup>4</sup> cells transferred) (Fig. 7B). This result indicated that in both groups protection was primarily mediated by CD8-T<sub>M</sub> cells specific for the collectivity of non-IDEs with no obvious improvement

made by the expansion of CD8-T<sub>M</sub> cells specific for conditional IDEs, the m145 epitope in the particular example.

As the “therapeutic increment” of adoptive cell transfer re-quires 10-fold differences in the numbers of transferred cells for effecting significant differences in protection (55;

see numerous subsequent reports reviewed in references 20, 22, and 49), our present findings do not mean that the expanded m145 epitope-specific CD8-T<sub>M</sub>-cell subset did not contribute at all to the protection mediated by the ΔIDE-primed population. Rather, the data show that its *in vivo* contribution was quantitatively too small to have had a measurable biological impact on the control of CMV disease. In any case, our data have shown that release from immunodomination by IDEs is not required for a substantial antiviral protection by a CD8-T<sub>M</sub>-cell population that represents the collectivity of non-IDEs encoded by a complex virus.

**Functional avidity may rearrange epitope hierarchies.** So far in this study, we have not yet considered a possible implication of TCR affinity for presented epitopes, one important parameter determining the functional avidity of CD8 T cells (reviewed in reference 28). Epitope immunodominance is usually defined by the response magnitude, that is, by the numerical pool size of CD8 T cells carrying cognate TCRs after priming and subsequent shaping of the memory repertoire. Protective immunity, however, does not necessarily correlate with the hierarchy of CD8 T-cell responses (14). It also does not strictly correlate with functional avidity, as low avidity may suffice for epitopes that are efficiently processed and presented while high avidity is more likely required for poorly processed and presented epitopes (1). In the specific case of mCMV, immunoevasin m152/gp40 was shown to abrogate the existing protective potential of numerically dominant CD8-T<sub>M</sub> cells by preventing the presentation of the corresponding M45-D<sup>b</sup> peptide (25). The inhibitory effect of immunoevasin m152, or of all three immunoevasins of mCMV combined, is less complete for all other mCMV epitopes tested (21), but it undoubtedly limits the presentation of naturally processed antigenic peptides in infected cells (Fig. 4). Therefore, “functional immunodominance” of epitopes in the antiviral effector phase might more closely be reflected by the frequencies of high-avidity CD8 T cells rather than by the total frequencies measured under *in vitro* conditions of optimal, but unphysiological, MHC-I loading with synthetic peptides. Specifically, CD8-T<sub>M</sub> cells with a functional avidity that is too low to detect naturally processed and presented peptide on infected cells *in vivo* will obviously not be able to contribute to protection.

In pursuing this idea, we determined the functional avidities of polyclonal *ex vivo* CD8-T<sub>M</sub> cells primed by mCMV-WT.BAC for selected epitopes of interest (Fig. 8). This comparison revealed that IDEs IE1 and m164 profited most from high concentrations of antigenic peptide, whereas the frequency of cells with high avidity was found to be higher for some of the non-IDEs (Fig. 8A). Specifically, the CD8 T-cell population contained CD8-T<sub>M</sub> cells capable of recognizing the M105 epitope at a peptide loading concentration at which IDE-specific CD8 T cells were barely detectable. In Fig. 8B, these data are rearranged to reveal more clearly how immunodominance hierarchy patterns can change, depending on peptide concentration. For instance, at 10<sup>-7</sup> M, IDE IE1 ranked as number 1 in the hierarchy, whereas it dropped back to rank number 2 and rank number 4 at peptide concentrations of 10<sup>-8</sup> and 10<sup>-9</sup> M, respectively. Finally, at 10<sup>-10</sup> M, M105 and m145 have to be classified as being IDEs. In conclusion, these data predict that under conditions of limited peptide presentation *in vivo*,

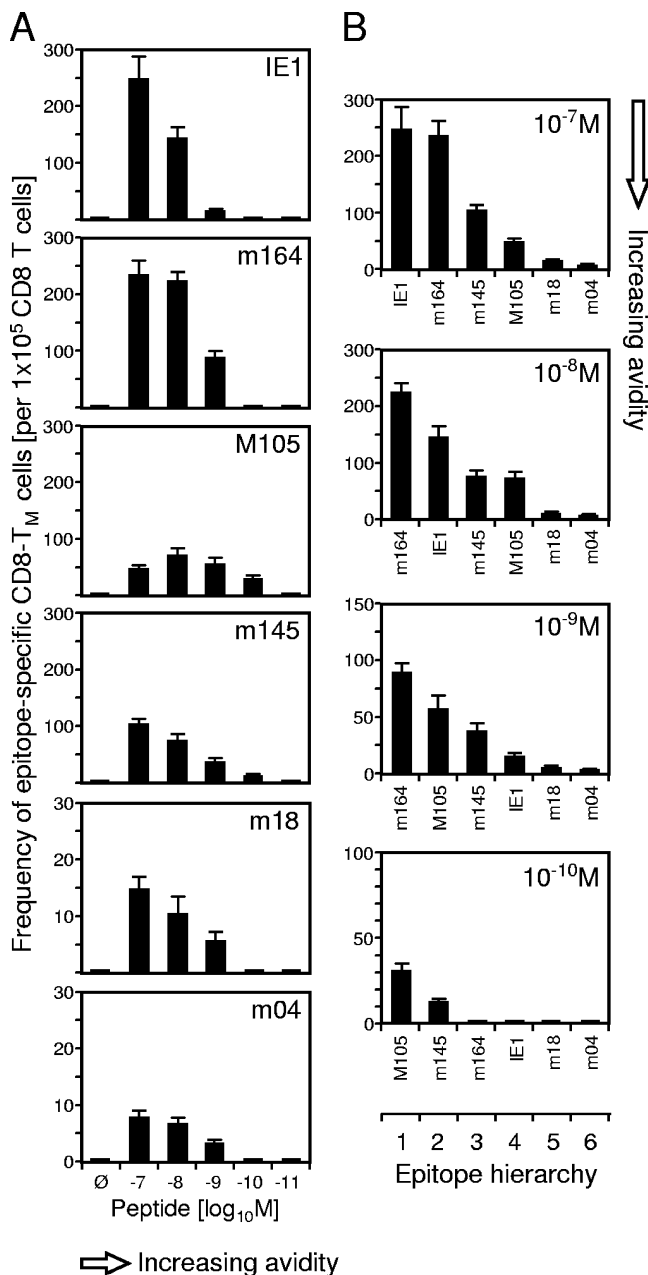


FIG. 8. Epitope-specific functional avidities of CD8-T<sub>M</sub> cells primed by mCMV-WT. (A) Frequencies dependent upon peptide concentration. (B) Immunodominance hierarchies of epitopes dependent upon peptide concentration. BALB/c mice were primed by infection with mCMV-WT.Smith, and 8 months later CD8 T cells were purified from a pool of 20 spleens. These cells were used as responder cells in an ELISPOT assay performed with P815 stimulator cells exogenously loaded with the indicated concentrations of synthetic antigenic peptides representing a selection of currently known H-2<sup>d</sup>-restricted mCMV-encoded epitopes. Bars represent the frequencies of responding CD8-T<sub>M</sub> cells. For error statistics, see the legend of Fig. 3. ∅, stimulator cells with no viral peptide added.

CD8-T<sub>M</sub> cells specific for IDEs are no longer superior to those specific for non-IDEs, neither quantitatively nor qualitatively. **Acquired numerical immunodominance of a conditional IDE based primarily on the expansion of intermediate-to-low-avidity CD8-T<sub>M</sub> cells.** The avidity data shown so far were based on

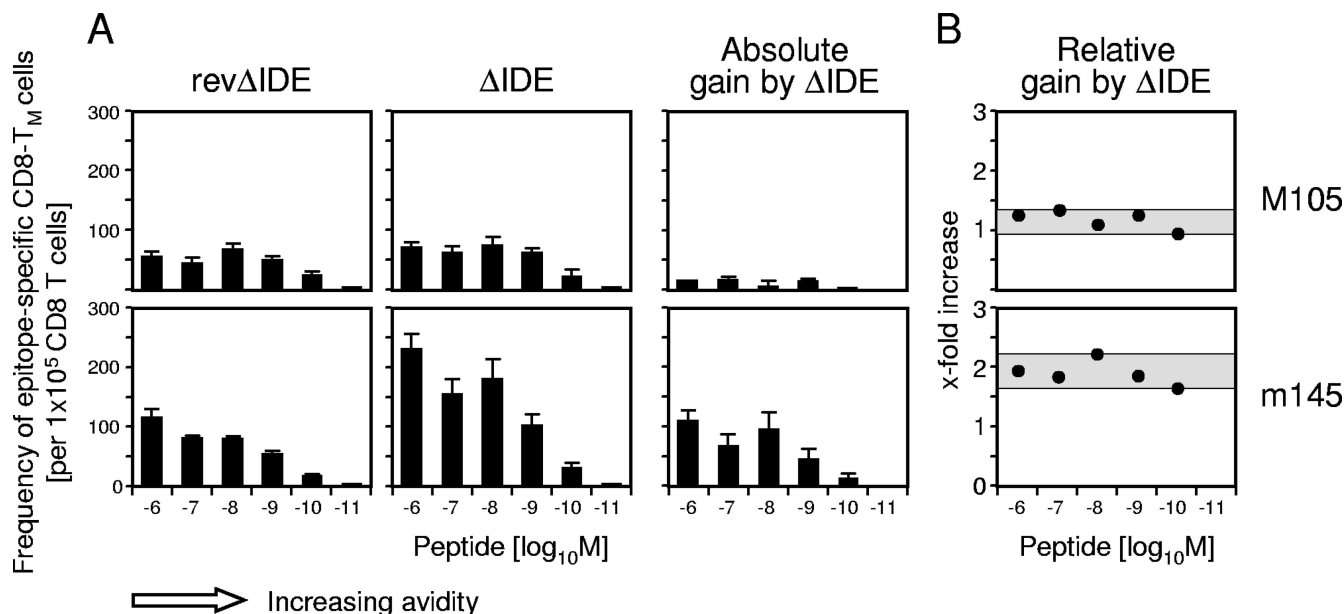


FIG. 9. Influence of IDE deletion on the frequencies and functional avidities of CD8-T<sub>M</sub> cells specific for non-IDEs M105 and m145. (A) Avidity-dependent absolute compensatory response to IDE deletion. CD8 T cells were purified from pools of 10 spleens per group at 6 months after priming of BALB/c mice by infection with mCMV-*rev*ΔIDE and mCMV-ΔIDE. This experiment was performed with memory cell donors from the batches of infected mice already used for the protection experiment shown in Fig. 7 so that functional avidities and protective antiviral effectiveness *in vivo* can be correlated. Bars represent the frequencies of responding CD8-T<sub>M</sub> cells. For error statistics, see the legend of Fig. 3. (B) Avidity-independent relative compensatory response to IDE deletion. Relative expansion of CD8-T<sub>M</sub> cell populations in the absence of IDEs is calculated as the quotient of ΔIDE and *rev*ΔIDE CD8-T<sub>M</sub>-cell frequencies. Avidity independence is highlighted by a gray-shaded zone representing the range of the factor of increase.

priming with mCMV-WT.BAC expressing IDEs IE1 and m164. Deletion of these two IDEs was shown to allow an expansion of CD8-T<sub>M</sub> cells specific for the m145 epitope (Fig. 5). This raised the question of whether deletion of constitutive IDEs has an influence also on the avidity distribution in the pool of CD8-T<sub>M</sub> cells specific for the remaining epitopes. One possibility was that absence of immunodomination by IDEs favors the expansion primarily of low-avidity CD8-T<sub>M</sub> cells specific for conditional IDEs. We have addressed this issue by comparing the functional avidities of CD8-T<sub>M</sub> cells primed by mCMV-*rev*ΔIDE and mCMV-ΔIDE for the epitopes M105 and m145 (Fig. 9). Again, in agreement with the ORF antigenicity screening data (Fig. 5), m145 rather than M105 profited from the deletion of constitutive IDEs.

Most importantly, this “acquired immunodominance” in absolute response magnitude was found to be based mainly on the expansion of intermediate-to-low avidity CD8-T<sub>M</sub> cells (Fig. 9A), although in relative terms m145-specific CD8-T<sub>M</sub> cells expanded twofold in the absence of IDEs independent of their functional avidity (Fig. 9B). Thus, while our data did not confirm the assumption that low-avidity CD8-T<sub>M</sub> cells would profit to an above average extent from the deletion of IDEs, the expanded m145-specific CD8-T<sub>M</sub>-cell population was comprised mainly of intermediate-to-low avidity CD8-T<sub>M</sub> cells. If we assume that peptide presentation is limited *in vivo*, which is reasonable as discussed above, this is one possible explanation why expansion of m145-specific CD8-T<sub>M</sub> cells contributed so little to protection.

## DISCUSSION

Here, we have analyzed a putative influence of immunodomination on the protective CD8-T<sub>M</sub>-cell response against a complex virus with high coding capacity, namely mCMV, a member of the herpesvirus family. As a valuable new tool, we generated mutant virus mCMV-ΔIDE. To the best of our knowledge, this is the first study to show the impact of deleting all immunodominant MHC-I memory repertoire epitopes of a herpesvirus for a certain MHC haplotype (*H-2<sup>d</sup>* in the specific example) on the shaping of a memory repertoire in general and on antiviral protection in a clinically relevant model in particular.

Our data have shown that deletion of IDEs from the viral proteome has remarkably little, if any, influence on the recognition of infected target cells and on *in vivo* antiviral protection by polyclonal *ex vivo* CD8-T<sub>M</sub> cells. It is currently widely assumed that deletion of IDEs is compensated for by expansion of cells specific for epitopes that were otherwise suppressed by immunodomination. In particular, for viruses with high coding capacity, candidate epitopes that might profit from an absence of IDEs are numerous. The new finding here is that this explanation does not apply to mCMV.

By employing a relatively new approach, namely, a viral genome-wide ORF library screening for antigenicity (41), we got the surprising result that deletion of IDEs does not induce global alterations in antigenic ORF usage but results in only minor adaptation of the memory epitope repertoire. None of the previously known epitopes profited significantly from the

deletion of IDEs, and only one out of a total of ~170 ORFs, namely, ORF *m145*, was found to contain a newly identified epitope for which cognate CD8-T<sub>M</sub> cells reproducibly expanded after deletion of IDEs. Moreover, the increase in frequency of m145-specific CD8-T<sub>M</sub> cells proved to result mainly from the expansion of cells with intermediate-to-low functional avidity. A correlation between functional avidity of CTL and antiviral protection has previously been indicated by studies on lymphocytic choriomeningitis virus (14). Accordingly, CD8-T<sub>M</sub> cells with low functional avidity are likely to contribute little to protection against mCMV under the in vivo conditions of limited peptide presentation.

The decisive experiment was the comparison of the protective effectiveness of donor CD8-T<sub>M</sub> cells primed with mCMV- $\Delta$ IDE and mCMV- $\Delta$ IDE upon adoptive transfer into immunocompromised recipients infected with mCMV- $\Delta$ IDE (Fig. 7). This experimental setting directly compared CD8-T<sub>M</sub> cells specific for non-IDEs "educated" in the presence of IDEs with those that have had the chance to expand in the absence of the postulated immunodominating effect of the IDEs. The key result is that CD8-T<sub>M</sub> cells with specificity for non-IDEs but primed under conditions of immunodomination by IDEs were fully protective against infection with mCMV- $\Delta$ IDE, thus demonstrating the collective protective potential of non-IDEs independent of release from immunodomination. This is an unexpected result not predicted by the literature.

The mechanism that leads to epitope immunodominance in terms of CD8 T-cell response magnitude is one of the open questions in immunology. So far, immunodominance could not be attributed to any single structural or functional property of the antigenic protein or the processed antigenic peptide but may rather result from a complex interplay of many parameters, eventually resulting in a proliferation advantage of CD8 T cells carrying TCRs specific for certain MHC-peptide complexes (9, 68, 69).

The murine model of CMV infection has demonstrated also that subdominant epitopes can elicit highly protective immunity. Two complementary lines of evidence have led to this conclusion, namely, DNA vaccination of the immunocompetent host and CD8 T-cell-based adoptive therapy in the immunocompromised host (for reviews, see references 20, 22, and 49).

As shown by D. H. Spector's group, DNA vaccination of BALB/c mice with expression plasmids encoding non-IDEs m04 (38) or M84 (36, 66, 67) protects as efficiently as the plasmid encoding IDE IE1/m123 (17, 66). Recent work from this group has demonstrated protection elicited by a plasmid encoding M105, the conserved mCMV homolog of hCMV UL105 (37). We have here independently identified a K<sup>d</sup>-presented peptide of M105 that elicits high-avidity CD8-T<sub>M</sub> cells. Most importantly, the DNA vaccination studies have documented that the epitope-specific response magnitude can exceed the response elicited by infection and that the response to non-IDEs can reach IDE levels.

Our own group's previous work has been focused on antiviral protection mediated by CD8 T cells specific for IDEs and non-IDEs upon adoptive transfer into immunocompromised recipients as a preclinical model for adoptive cytoimmuno-therapy of CMV disease (reviewed in references 20 and 22). In essence, the message of these studies is that epitope-specific

CTLL generated from ex vivo CD8-T<sub>M</sub> cells are protective regardless of whether they are specific for IDEs IE1 and m164 (27) or non-IDEs m04 (26), m18 (22), M45-D<sup>d</sup> (R. H., unpublished data), M83 (24), and M84 (24). This indicated a sufficient in vivo presentation of these epitopes. As an extreme counterexample, CTLL as well as sort-purified ex vivo CD8-T<sub>M</sub> cells specific for an immunodominant M45-D<sup>b</sup> epitope (16) failed to protect C57BL/6 recipients because presentation of this particular peptide is prevented by immunoevasin m152 in infected host tissue cells (25).

Altogether, both of these approaches concurred in the conclusion that the immunodominance hierarchy rank of an epitope does not predict the relevance of the respective CD8 T cells in the antiviral effector phase of the immune response. Although these previous findings are of relevance for interventional strategies, one must take into account that DNA vaccination with a non-IDE expands the cognate CD8 T cells to levels not reached during infection (66). Likewise, in the case of adoptive transfer of epitope-specific CTLL or TCR-sorted ex vivo CD8-T<sub>M</sub> cells, all cells are specific for the chosen epitope. In the context of infection, however, non-IDEs with a per-cell protective potential comparable to that of IDEs may nevertheless be inferior to IDEs simply because of the low number of cognate CD8 T cells maintained during memory.

Our study refers to the memory repertoire that is shaped not only by the initial priming event but also by subsequent selection. It has been shown previously that memory repertoires are more focused than acute response repertoires, with CD8-T<sub>M</sub> cells specific for IE1 and m164 dominating in BALB/c (27) and CD8-T<sub>M</sub> cells specific for five epitopes, including two epitopes in IE3, dominating in C57BL/6 mice (40). These findings in the two most extensively studied mouse models of CMV infection compare well to the hCMV-specific CD8-T<sub>M</sub>-cell repertoires in humans that were found to be focused on between 1 and 32 antigenic ORFs, with a median value of 8 ORFs among 33 CMV-seropositive, healthy volunteers included in the trial (61). Notably, hCMV IE2 (the homolog of mCMV IE3) and IE1 were among the most prevalent hCMV ORFs recognized by CD8-T<sub>M</sub> cells in humans, suggesting that IE proteins play an above average role in shaping CMV-specific memory repertoires. This may relate to the recent finding that in the BALB/c model, desilencing of IE genes during viral latency can lead to in situ restimulation of IE1-specific CD8-T<sub>M</sub> cells (23, 58; for a review, see reference 59). Thus, our observations might reflect, in part, the specific biology of CMVs in that only non-IDEs for which the corresponding genes are expressed during viral latency can take long-term advantage of the deletion of IDEs.

That deletion of IDEs in viral genomes can lead to expansion of CD8 T cells specific for epitopes that are otherwise non-IDEs is known, however, also from other infection models. In CTL escape variants of lymphocytic choriomeningitis virus, for instance, mutational loss of all three IDEs, GP1, GP2, and NP, was found to be compensated for by a protective CTL response against the L protein that was not known before as an antigen for CTL (33); another study, however, showed that combined loss of IDEs GP1 and GP2 was associated with a markedly reduced CTL response and a less efficient control of infection in vivo (39). Mylin and colleagues (42) found a response to a D<sup>b</sup>-restricted epitope in SV40 T antigen only

with an epitope loss virus variant lacking the three IDEs present in the T antigen. Along the same line of evidence, deletion of an IDE in the nucleoprotein of influenza virus PR8 by MHC anchor residue mutation led to an expansion of CTL specific for non-IDEs present in the same protein (12). Collectively, these findings led to the conclusion that CTL epitopes form a hierarchy in which responses to weak epitopes are suppressed in the presence of stronger epitopes (33), which led to the concept of immunodomination.

From the literature on other viruses discussed above, one would have predicted that deletion of the two IDEs IE1 and m164 of mCMV is of limited significance for protection, as the host can mount a compensatory response directed against non-IDEs. While the first part of the prediction proved to be true, the second part did not apply. A possible explanation may lie in the CD8-T<sub>M</sub>-cell avidity distributions. Our study has revealed that numerical immunodominance of the mCMV IDEs is based primarily on a high proportion of low-avidity CD8-T<sub>M</sub> cells, whereas the frequencies of high-avidity CD8-T<sub>M</sub> cells—capable of detecting small amounts of presented peptide—were less different between IDEs and non-IDEs. This does in no way mean that IDE-specific CD8-T<sub>M</sub> cells are always of low avidity. Our previous work has clearly shown the existence of protective high-avidity CD8-T<sub>M</sub> cells specific for IDE IE1 (44). One must also consider the possibility of a dynamics of the avidity distribution in the course of infection. What our findings tell us is that the advantage of IDEs over non-IDEs vanishes under conditions of limited peptide presentation. Thus, at least for mCMV, a central postulate of the concept of immunodomination, namely, that IDEs are strong and non-IDEs are weak epitopes on principle (33), does not hold true in terms of functional avidity and protective potential.

Besides the more basic research interest in the general rules of IDE hierarchies, our study could also have implications for adoptive immunotherapy of CMV disease in HSCT patients who receive donor lymphocytes primed by a CMV variant that is antigenically distinct from the reactivating endogenous CMV variant (see introduction). We have used here adoptive transfer in the immunocompromised BALB/c mouse as a preclinical model for investigating two D<sup>Var1</sup>R<sup>Var2</sup> constellations with antigenic mismatch, namely, the constellations D<sup>AIDE</sup>R<sup>IDE</sup> and D<sup>IDE</sup>R<sup>AIDE</sup>. It is important to point out that CMV-specific donor cells in clinical HSCT are always memory cells, since persons with acute CMV infection can, of course, not donate stem cells or T cells. Our preclinical model took this into account by using CD8-T<sub>M</sub> cells for the adoptive transfer. For the constellation D<sup>AIDE</sup>R<sup>IDE</sup>, our data predict that lack of IDEs in the specificity repertoire of donor-derived CD8-T<sub>M</sub> cells will not severely diminish the therapeutic antiviral efficacy. From a clinician's point of view, the inverse case of a recipient infected with a CMV variant lacking IDEs expressed by the CMV variant of the donor, that is, the D<sup>IDE</sup>R<sup>AIDE</sup> constellation, is even more relevant as potential donors can be pretested and selected for the presence of IDEs, whereas the patient's CMV variant has to be accepted as given. It is therefore of interest that our data suggest, somewhat unexpectedly, that this constellation should pose no real problem.

In conclusion, the model predicts that the success of CD8 T-cell therapy of CMV in HSCT recipients will not be severely

affected by even major antigenic differences between virus variants.

#### ACKNOWLEDGMENTS

This work was supported by the Deutsche Forschungsgemeinschaft, SFB 490, individual projects E2 (C.O.S., M.J.R., and N.K.A.G.), E3 (R.H. and P.D.), and E4 (T.D., S.F.E., S.A.O.-K., and M.J.R.) as well as the Clinical Research Group KFO 183, individual project TP8, Establishment of a challenge model to optimize the immunotherapy of cytomegalovirus diseases (M.J.R.). Further support was provided by the Ministry of Science of the Federal State Rheinland-Pfalz, Immunology Cluster of Excellence Immunointervention. The contributions of M.W.M. and A.B.H. were supported by NIH grants R01 AI47206 and R01 AI50099 as well as by NIH training grant 5T32 AI007472. Special thanks go to the Gerhard and Martha Röttger-Stiftung and the Hans-Joachim und Ilse Brede Stiftung for generous donations.

#### REFERENCES

- Alexander-Miller, M. A., G. R. Leggatt, and J. A. Berzofsky. 1996. Selective expansion of high- or low-avidity cytotoxic lymphocytes and efficacy for adoptive immunotherapy. *Proc. Natl. Acad. Sci. USA* **93**:4102–4107.
- Appelbaum, F. R. 2001. Haematopoietic cell transplantation as immunotherapy. *Nature* **411**:385–389.
- Böhm, V., J. Podlech, D. Thomas, P. Deegen, M.-F. Pahl-Seibert, N. A. W. Lemmermann, N. K. A. Grzimek, S. A. Oehrlein-Karpi, M. J. Reddehase, and R. Holtappels. 2008. Epitope-specific in vivo protection against cytomegalovirus disease by CD8 T cells in the murine model of preemptive immunotherapy. *Med. Microbiol. Immunol.* **197**:135–144.
- Borst, E. M., G. Hahn, U. H. Koszinowski, and M. Messerle. 1999. Cloning of the human cytomegalovirus (HCMV) genome as an infectious bacterial artificial chromosome in *Escherichia coli*: a new approach for construction of HCMV mutants. *J. Virol.* **73**:8320–8329.
- Borst, E. M., G. Posfai, F. Pogoda, and M. Messerle. 2004. Mutagenesis of herpesvirus BACs by allele replacement. *Methods Mol. Biol.* **256**:269–279.
- Britt, W. 2006. Human cytomegalovirus infections and mechanisms of disease, p. 1–28. *In* M. J. Reddehase (ed.), *Cytomegaloviruses: molecular biology and immunology*. Caister Academic Press, Wymondham, Norfolk, United Kingdom.
- Brune, W., M. Wagner, and M. Messerle. 2006. Manipulating cytomegalovirus genomes by BAC mutagenesis: strategies and applications, p63–89. *In* M. J. Reddehase (ed.), *Cytomegaloviruses: molecular biology and immunology*. Caister Academic Press, Wymondham, Norfolk, United Kingdom.
- Bunde, T., A. Kirchner, B. Hoffmeister, D. Habedank, R. Hetzer, G. Cherepnev, S. Prösch, P. Reinke, H. D. Volk, H. Lehmkuhl, and F. Kern. 2005. Protection from cytomegalovirus after transplantation is correlated with immediate early 1-specific CD8 T cells. *J. Exp. Med.* **201**:1031–1036.
- Chen, W., L. C. Anton, J. R. Bennink, and J. W. Yewdell. 2000. Dissecting the multifactorial causes of immunodominance in class I-restricted T cell responses to viruses. *Immunity* **12**:83–93.
- Cobbold, M., N. Khan, B. Pourghesari, S. Tauro, D. McDonald, H. Osman, M. Assenmacher, I. Billingham, C. Steward, C. Crawley, E. Olavarria, J. Goldman, R. Chakraverty, P. Mahendra, C. Craddock, and P. A. Moss. 2005. Adoptive transfer of cytomegalovirus-specific CTL to stem cell transplant patients after selection by HLA-peptide tetramers. *J. Exp. Med.* **202**:379–386.
- Darlington, J., M. Super, K. Patel, J. E. Grundy, P. D. Griffiths, and V. C. Emery. 1991. Use of the polymerase chain reaction to analyse sequence variation within a major neutralizing epitope of glycoprotein B (gp58) in clinical isolates of human cytomegalovirus. *J. Gen. Virol.* **72**:1985–1989.
- Deng, Y., J. W. Yewdell, L. C. Eisenlohr, and J. R. Bennink. 1997. MHC affinity, peptide liberation, T cell repertoire, and immunodominance all contribute to the paucity of MHC class I-restricted peptides recognized by antiviral CTL. *J. Immunol.* **158**:1507–1515.
- Emery, V. C. 1998. Relative importance of cytomegalovirus load as a risk factor for cytomegalovirus disease in the immunocompromised host, p. 288–301. *In* M. Scholz, H. F. Rabenau, H. W. Doerr, and J. Cinatl, Jr. (ed.), *CMV-related immunopathology*. Monographs in virology, vol. 21. Karger, Basel, Switzerland.
- Gallimore, A., T. Dumrese, H. Hengartner, R. M. Zinkernagel, and H. G. Rammensee. 1998. Protective immunity does not correlate with the hierarchy of virus-specific cytotoxic T cell responses to naturally processed peptides. *J. Exp. Med.* **187**:1647–1657.
- Ghazal, P., M. Messerle, K. Osborn, and A. Angulo. 2003. An essential role of the enhancer for murine cytomegalovirus in vivo growth and pathogenesis. *J. Virol.* **77**:3217–3228.
- Gold, M. C., M. W. Munks, M. Wagner, U. H. Koszinowski, A. B. Hill, and S. P. Fling. 2002. The murine cytomegalovirus immunomodulatory gene *m152* prevents recognition of infected cells by M45-specific CTL, but does

- not alter the immunodominance of the M45-specific CD8 T cell response in vivo. *J. Immunol.* **169**:359–365.
17. **Gonzales Armas, J. C., C. S. Morello, L. D. Cranmer, and D. H. Spector.** 1996. DNA immunization confers protection against murine cytomegalovirus infection. *J. Virol.* **70**:7921–7928.
  18. **Hebart, H., and H. Einsele.** 2004. Clinical aspects of CMV infection after stem cell transplantation. *Hum. Immunol.* **65**:432–436.
  19. **Ho, S. N., H. D. Hunt, R. M. Horton, J. K. Pullen, and L. R. Pease.** 1989. Site-directed mutagenesis by overlap extension using the polymerase chain reaction. *Gene* **77**:51–59.
  20. **Holtappels, R., V. Böhm, J. Podlech, and M. J. Reddehase.** 2008. CD8 T-cell-based immunotherapy of cytomegalovirus infection: “proof of concept” provided by the murine model. *Med. Microbiol. Immunol.* **197**:125–134.
  21. **Holtappels, R., D. Gillert-Marién, D. Thomas, J. Podlech, P. Deegen, S. Herter, S. A. Oehrlein-Karpi, D. Strand, M. Wagner, and M. J. Reddehase.** 2006. Cytomegalovirus encodes a positive regulator of antigen presentation. *J. Virol.* **80**:7613–7624.
  22. **Holtappels, R., M. W. Munks, J. Podlech, and M. J. Reddehase.** 2006. CD8 T-cell-based immunotherapy of cytomegalovirus disease in the mouse model of the immunocompromised bone marrow transplantation recipient, p. 383–418. *In* M. J. Reddehase (ed.), *Cytomegaloviruses: molecular biology and immunology*. Caister Academic Press, Wymondham, Norfolk, United Kingdom.
  23. **Holtappels, R., M.-F. Pahl-Seibert, D. Thomas, and M. J. Reddehase.** 2000. Enrichment of immediate-early 1 (*mI23/pp89*) peptide-specific CD8 T cells in a pulmonary CD62L<sup>lo</sup> memory-effector cell pool during latent murine cytomegalovirus infection of the lungs. *J. Virol.* **74**:11495–11503.
  24. **Holtappels, R., J. Podlech, N. K. A. Grzimek, D. Thomas, M.-F. Pahl-Seibert, and M. J. Reddehase.** 2001. Experimental preemptive immunotherapy of murine cytomegalovirus disease with CD8 T-cell lines specific for ppM83 and ppM84, the two homologs of human cytomegalovirus tegument protein ppUL83 (pp65). *J. Virol.* **75**:6584–6600.
  25. **Holtappels, R., J. Podlech, M.-F. Pahl-Seibert, M. Juelch, D. Thomas, C. O. Simon, M. Wagner, and M. J. Reddehase.** 2004. Cytomegalovirus misleads its host by priming of CD8 T cells specific for an epitope not presented in infected tissues. *J. Exp. Med.* **199**:131–136.
  26. **Holtappels, R., D. Thomas, J. Podlech, G. Geginat, H.-P. Steffens, and M. J. Reddehase.** 2000. The putative natural killer decoy early gene *m04* (gp34) of murine cytomegalovirus encodes an antigenic peptide recognized by protective antiviral CD8 T cells. *J. Virol.* **74**:1871–1884.
  27. **Holtappels, R., D. Thomas, J. Podlech, and M. J. Reddehase.** 2002. Two antigenic peptides from genes *m123* and *m164* of murine cytomegalovirus quantitatively dominate CD8 T-cell memory in the *H-2<sup>d</sup>* haplotype. *J. Virol.* **76**:151–164.
  28. **Kedl, R. M., J. W. Kappler, and P. Marrack.** 2003. Epitope dominance, competition and T cell affinity maturation. *Curr. Opin. Immunol.* **15**:120–127.
  29. **Kolb, H. J., B. Simoes, and C. Schmid.** 2004. Cellular immunotherapy after allogeneic stem cell transplantation in hematologic malignancies. *Curr. Opin. Oncol.* **16**:167–173.
  30. **Krmpotic, A., M. Hasan, A. Loewendorf, T. Saulig, A. Halenius, T. Lenac, B. Polic, I. Bubic, A. Kriegeskorte, E. Pernjak-Pugel, M. Messerle, H. Hengel, D. H. Busch, U. H. Koszinowski, and S. Jonjic.** 2005. NK cell activation through the NKG2D ligand MULT-1 is selectively prevented by the glycoprotein encoded by mouse cytomegalovirus gene *m145*. *J. Exp. Med.* **201**:211–220.
  31. **Kurz, S. K., H.-P. Steffens, A. Mayer, J. R. Harris, and M. J. Reddehase.** 1997. Latency versus persistence or intermittent recurrences: evidence for a latent state of murine cytomegalovirus in the lungs. *J. Virol.* **71**:2980–2987.
  32. **Lazzarotto, T., M. C. Bocconi, P. Dal Monte, A. Ripalti, and M. P. Landini.** 1991. Antigenic variation of cytomegalovirus isolates recovered from infected children. *Microbiologica* **14**:241–251.
  33. **Lewicki, H. A., M. G. von Herrath, C. F. Evans, J. L. Whitton, and M. B. Oldstone.** 1995. CTL escape viral variants. II. Biologic activity in vivo. *Virology* **211**:443–450.
  34. **Lyons, P. A., J. E. Allan, C. Carrello, G. R. Shellam, and A. A. Scalzo.** 1996. Effect of natural sequence variation at the H-2L<sup>d</sup>-restricted CD8<sup>+</sup> T cell epitope of the murine cytomegalovirus *ie1*-encoded pp89 on T cell recognition. *J. Gen. Virol.* **77**:2615–2623.
  35. **Messerle, M., I. Crnkovic, W. Hammerschmidt, H. Ziegler, and U. H. Koszinowski.** 1997. Cloning and mutagenesis of a herpesvirus genome as an infectious bacterial artificial chromosome. *Proc. Natl. Acad. Sci. USA* **94**:14759–14763.
  36. **Morello, C. S., L. D. Cranmer, and D. H. Spector.** 2000. Suppression of murine cytomegalovirus (MCMV) replication with a DNA vaccine encoding MCMV M84 (a homolog of human cytomegalovirus pp65). *J. Virol.* **74**:3696–3708.
  37. **Morello, C. S., L. A. Kelley, M. W. Munks, A. B. Hill, and D. H. Spector.** 2007. DNA immunization using the highly conserved murine cytomegalovirus genes encoding the homologs of human cytomegalovirus UL54 (DNA polymerase) and UL105 (helicase) elicits strong CD8 T-cell responses and is protective against systemic challenge. *J. Virol.* **81**:7766–7775.
  38. **Morello, C. S., M. Ye, and D. H. Spector.** 2002. Development of a vaccine against murine cytomegalovirus (MCMV) consisting of plasmid DNA and formalin-inactivated MCMV, that provides long-term, complete protection against viral replication. *J. Virol.* **76**:4822–4835.
  39. **Moskophidis, D., and R. M. Zinkernagel.** 1995. Immunobiology of cytotoxic T-cell escape mutants of lymphocytic choriomeningitis virus. *J. Virol.* **69**:2187–2193.
  40. **Munks, M. W., K. S. Cho, A. K. Pinto, S. Sierro, P. Klenerman, and A. B. Hill.** 2006. Four distinct patterns of memory CD8 T cell responses to chronic murine cytomegalovirus infection. *J. Immunol.* **177**:450–458.
  41. **Munks, M. W., M. C. Gold, A. L. Zajac, C. M. Doom, C. S. Morello, D. H. Spector, and A. B. Hill.** 2006. Genome-wide analysis reveals a highly diverse CD8 T cell response to murine cytomegalovirus. *J. Immunol.* **176**:3760–3766.
  42. **Mylin, L. M., R. H. Bonneau, J. D. Lippolis, and S. S. Tevethia.** 1995. Hierarchy among multiple H-2<sup>b</sup>-restricted cytotoxic T-lymphocyte epitopes within simian virus 40 T antigen. *J. Virol.* **69**:6665–6677.
  43. **O'Connor, M., M. Peifer, and W. Bender.** 1989. Construction of large DNA segments in *Escherichia coli*. *Science* **244**:1307–1312.
  44. **Pahl-Seibert, M.-F., M. Juelch, J. Podlech, D. Thomas, P. Deegen, M. J. Reddehase, and R. Holtappels.** 2005. Highly protective in vivo function of cytomegalovirus IE1 epitope-specific memory CD8 T cells purified by T-cell receptor-based cell sorting. *J. Virol.* **79**:5400–5413.
  45. **Peggs, K. S., S. Verfuërth, A. Pizzey, N. Khan, M. Gulver, P. A. Moss, and S. Mackinnon.** 2003. Adoptive cellular therapy for early cytomegalovirus infection after allogeneic stem-cell transplantation with virus-specific T-cell lines. *Lancet* **362**:1375–1377.
  46. **Podlech, J., R. Holtappels, N. K. A. Grzimek, and M. J. Reddehase.** 2002. Animal models: murine cytomegalovirus, p. 493–525. *In* S. H. E. Kaufmann and D. Kabelitz (ed.), *Methods in microbiology: immunology of infection*, 2nd ed., vol. 32. Academic Press, London, United Kingdom.
  47. **Posfai, G., M. D. Koob, H. A. Kirkpatrick, and F. R. Blattner.** 1997. Versatile insertion plasmids for targeted genome manipulations in bacteria: isolation, deletion, and rescue of the pathogenicity island LEE of the *Escherichia coli* O157:H7 genome. *J. Bacteriol.* **179**:4426–4428.
  48. **Rawlinson, W. D., H. E. Farrell, and B. G. Barrrell.** 1996. Analysis of the complete DNA sequence of murine cytomegalovirus. *J. Virol.* **70**:8833–8849.
  49. **Reddehase, M. J.** 2002. Antigens and immunoevasins: opponents in cytomegalovirus immune surveillance. *Nature Rev. Immunol.* **2**:831–844.
  50. **Reddehase, M. J., S. Jonjic, F. Weiland, W. Mutter, and U. H. Koszinowski.** 1988. Adoptive immunotherapy of murine cytomegalovirus adenitis in the immunocompromised host: CD4-helper-independent antiviral function of CD8-positive memory T lymphocytes derived from latently infected donors. *J. Virol.* **62**:1061–1065.
  51. **Reddehase, M. J., G. M. Keil, and U. H. Koszinowski.** 1984. The cytolytic T lymphocyte response to the murine cytomegalovirus. I. Distinct maturation stages of cytolytic T lymphocytes constitute the cellular immune response during acute infection of mice with the murine cytomegalovirus. *J. Immunol.* **132**:482–489.
  52. **Reddehase, M. J., and U. H. Koszinowski.** 1991. Redistribution of critical major histocompatibility complex and T cell receptor-binding functions of residues in an antigenic sequence after biterminal substitution. *Eur. J. Immunol.* **21**:1697–1701.
  53. **Reddehase, M. J., W. Mutter, and U. H. Koszinowski.** 1987. In vivo application of recombinant interleukin 2 in the immunotherapy of established cytomegalovirus infection. *J. Exp. Med.* **165**:650–656.
  54. **Reddehase, M. J., J. B. Rothbard, and U. H. Koszinowski.** 1989. A pentapeptide as minimal antigenic determinant for MHC class I-restricted T lymphocytes. *Nature* **337**:651–653.
  55. **Reddehase, M. J., F. Weiland, K. Münch, S. Jonjic, A. Lüske, and U. H. Koszinowski.** 1985. Interstitial murine cytomegalovirus pneumonia after irradiation: characterization of cells that limit viral replication during established infection of the lungs. *J. Virol.* **55**:264–273.
  56. **Riddell, S. R.** 1995. Pathogenesis of cytomegalovirus pneumonia in immunocompromised hosts. *Semin. Respir. Infect.* **10**:199–208.
  57. **Riddell, S. R., K. S. Watanabe, J. M. Goodrich, C. R. Li, M. E. Agha, and P. D. Greenberg.** 1992. Restoration of viral immunity in immunodeficient humans by the adoptive transfer of T cell clones. *Science* **257**:238–241.
  58. **Simon, C. O., R. Holtappels, H.-M. Tervo, V. Böhm, T. Däubner, S. A. Oehrlein-Karpi, B. Kühnappel, A. Renzaho, D. Strand, J. Podlech, M. J. Reddehase, and N. K. A. Grzimek.** 2006. CD8 T cells control cytomegalovirus latency by epitope-specific sensing of transcriptional reactivation. *J. Virol.* **80**:10436–10456.
  59. **Simon, C. O., C. K. Seckert, N. K. A. Grzimek, and M. J. Reddehase.** 2006. Murine model of cytomegalovirus latency and reactivation: the silencing/desilencing and immune sensing hypothesis, p. 483–500. *In* M. J. Reddehase (ed.), *Cytomegaloviruses: molecular biology and immunology*. Caister Academic Press, Wymondham, Norfolk, United Kingdom.
  60. **Steffens, H.-P., S. Kurz, R. Holtappels, and M. J. Reddehase.** 1998. Preemptive CD8 T-cell immunotherapy of acute cytomegalovirus infection prevents

- lethal disease, limits the burden of latent viral genomes, and reduces the risk of virus recurrence. *J. Virol.* **72**:1797–1804.
61. **Sylwester, A. W., B. L. Mitchell, J. B. Edgar, C. Taormina, C. Pelte, F. Ruchti, P. R. Sleath, K. H. Grabstein, N. A. Hosken, F. Kern, J. A. Nelson, and L. J. Picker.** 2005. Broadly targeted human cytomegalovirus-specific CD4<sup>+</sup> and CD8<sup>+</sup> T cells dominate the memory compartments of exposed subjects. *J. Exp. Med.* **202**:673–685.
  62. **Wagner, M., A. Gutermann, J. Podlech, M. J. Reddehase, and U. H. Koszinowski.** 2002. MHC class I allele-specific cooperative and competitive interactions between immune evasion proteins of cytomegalovirus. *J. Exp. Med.* **196**:805–816.
  63. **Wagner, M., S. Jonjic, U. H. Koszinowski, and M. Messerle.** 1999. Systematic excision of vector sequences from the BAC-cloned herpesvirus genome during virus reconstitution. *J. Virol.* **73**:7056–7060.
  64. **Walter, E. A., P. D. Greenberg, M. J. Gilbert, R. J. Finch, K. S. Watanabe, E. D. Thomas, and S. R. Riddell.** 1995. Reconstitution of cellular immunity against cytomegalovirus in recipients of allogeneic bone marrow by transfer of T-cell clones from the donor. *N. Engl. J. Med.* **333**:1038–1044.
  65. **Wills, M. R., A. J. Carmichael, and J. G. P. Sissons.** 2006. Adaptive cellular immunity to human cytomegalovirus, p. 341–365. *In* M. J. Reddehase (ed.), *Cytomegaloviruses: molecular biology and immunology*. Caister Academic Press, Wymondham, Norfolk, United Kingdom.
  66. **Ye, M., C. S. Morello, and D. H. Spector.** 2002. Strong CD8 T-cell responses following coimmunization with plasmids expressing the dominant pp89 and subdominant M84 antigens of murine cytomegalovirus correlate with long-term protection against subsequent viral challenge. *J. Virol.* **76**:2100–2112.
  67. **Ye, M., C. S. Morello, and D. H. Spector.** 2004. Multiple epitopes in the murine cytomegalovirus early gene product M84 are efficiently presented in infected primary macrophages and contribute to strong CD8<sup>+</sup> T-lymphocyte responses and protection following DNA immunization. *J. Virol.* **78**:11233–11245.
  68. **Yewdell, J. W.** 2006. Confronting complexity: real-world immunodominance in antiviral CD8<sup>+</sup> T cell responses. *Immunity* **25**:533–543.
  69. **Yewdell, J. W., and M. Del Val.** 2004. Immunodominance in TCD8<sup>+</sup> responses to viruses: cell biology, cellular immunology, and mathematical models. *Immunity* **21**:149–153.